Naval Research Laboratory

Washington, DC 20375-5320

NRL/MR/6180--06-8937

The Development of Advanced Sensor Technologies to Measure Critical Navy Mobility Fuel Properties

Robert E. Morris
Kevin J. Johnson
Mark H. Hammond
Susan L. Rose-Pehrsson

Navy Technology Center for Safety and Survivability
Chemistry Division

January 27, 2006

REPORT DOCUMENTATION PAGE

Form Approved
OMB No. 0704-0188

1. REPORT DATE *(DD-MM-YYYY)*	**2. REPORT TYPE**	**3. DATES COVERED** *(From - To)*
27-01-2006	Memorandum Report	September 2003 - September 2005

4. TITLE AND SUBTITLE

The Development of Advanced Sensor Technologies to Measure Critical Navy Mobility Fuel Properties

5a. CONTRACT NUMBER

5b. GRANT NUMBER

5c. PROGRAM ELEMENT NUMBER

6. AUTHOR(S)

Robert E. Morris, Kevin J. Johnson, Mark H. Hammond, and Susan L. Rose-Pehrsson

5d. PROJECT NUMBER

5e. TASK NUMBER
61-M850-B-6

5f. WORK UNIT NUMBER

7. PERFORMING ORGANIZATION NAME(S) AND ADDRESS(ES)

Naval Research Laboratory, Code 6180
4555 Overlook Avenue, SW
Washington, DC 20375-5320

8. PERFORMING ORGANIZATION REPORT NUMBER

NRL/MR/6180--06-8937

9. SPONSORING / MONITORING AGENCY NAME(S) AND ADDRESS(ES)

Naval Air Systems Command
Fuels and Lubricants Division, Air 4.4.5
22229 Elmer Road, Unit 4
Patuxent River, MD 20670-1534

10. SPONSOR / MONITOR'S ACRONYM(S)

NAVAIR

11. SPONSOR / MONITOR'S REPORT NUMBER(S)

12. DISTRIBUTION / AVAILABILITY STATEMENT

Approved for public release; distribution is unlimited.

13. SUPPLEMENTARY NOTES

14. ABSTRACT

Laboratory studies have been conducted at the Naval Research Laboratory (NRL) to develop chemometric methodologies and assess measurement technologies that will enable the implementation of sensor-based instrumentation capable of measuring critical Navy mobility fuel properties. These chemometric techniques were then used to evaluate several chromatographic and spectroscopic methods for their efficacy in modeling critical fuel properties. The preliminary findings from a training set consisting of 46 jet fuels from around the world, indicated that while capillary gas chromatography (GC) offered some advantages for certain properties, both near-IR (NIR) and Raman spectroscopy showed promise as suitable methods for a sensor-based analytical system. In many cases, the errors of prediction from partial least squares (PLS) regressions of the spectroscopic data were within the published errors of the standard ASTM test methods currently employed.

15. SUBJECT TERMS

Mobility fuel	Sensors	JP-5	F-76	Chemometrics	N-PLS	NIR	PLS	PARAFAC
Jet fuel	Fuel	JP-8	Naval distillate	Modeling	GC-MS	Raman	ANOVA	

16. SECURITY CLASSIFICATION OF:			**17. LIMITATION OF ABSTRACT**	**18. NUMBER OF PAGES**	**19a. NAME OF RESPONSIBLE PERSON**
a. REPORT	**b. ABSTRACT**	**c. THIS PAGE**			Robert E. Morris
Unclassified	Unclassified	Unclassified	UL	54	**19b. TELEPHONE NUMBER** *(include area code)* (202) 767-3845

Standard Form 298 (Rev. 8-98)
Prescribed by ANSI Std. Z39.18

CONTENTS

FIGURES

Figure

TABLES

Table

THE DEVELOPMENT OF ADVANCED SENSOR TECHNOLOGIES TO MEASURE CRITICAL NAVY MOBILITY FUEL PROPERTIES

1.0 SUMMARY

Current mobility fuel acceptance is performed in the shipboard fuel laboratory with a series of traditional fuel measurements. A fully automated, sensor-based analytical capability would offer significant savings in manpower and consumables, as well as provide for a safer, more rapid, and possibly more accurate analysis. Laboratory studies have thus been undertaken at the Naval Research Laboratory to develop chemometric methodologies and to assess measurement technologies that will enable the implementation of sensor-based instrumentation capable of measuring critical Navy mobility fuel properties.

One-dimensional and multi-way chemometric methods were developed to characterize trace level compositional changes occurring in fuels during aging or thermal degradation from gas chromatography (GC) and combined gas chromatography-mass spectrometry (GC-MS) analyses. Multi-way analysis of GC-MS data was also shown to be an extremely sensitive and effective method for elucidating the composition of trace fuel contaminants. These chemometric techniques were then used to evaluate several chromatographic and spectroscopic methods for their efficacy in modeling critical fuel properties.

The preliminary findings from a small training set consisting of 46 jet fuels from around the world, demonstrated the feasibility of performing quality assurance testing of shipboard fuels from either GC, near-IR (NIR) or Raman spectroscopy. GC offered certain advantages for some properties, and a data fusion approach in which both chromatography and spectroscopy are combined into one model may provide the means with which to confirm the presence of required fuel additives. In many cases, the errors of prediction from partial least squares (PLS) regressions were within the published errors of the standard ASTM test methods currently employed. However, in order to attain the necessary robustness of the predictive models, many more samples will need to be incorporated into the training set. Once a sufficient number of training set samples have been analyzed, the resulting property models can be incorporated into a stand-alone software application for evaluation by other Navy fuel laboratories. These models would form the basis for the design of a prototype sensor-based "black box" device to replace the current ASTM shipboard fuel quality acceptance test procedures.

2.0 INTRODUCTION

Hydrocarbon fuels are complex mixtures of organic compounds that are manufactured to comply with performance specifications based on properties, and not on composition. Thus while it is true that fuels obtained in conformance with a particular specification may be similar in their physical properties and performance, their composition may differ in both obvious and subtle ways. These compositional differences are a consequence of many factors which include refining and finishing methods, crude sources, handling methods, contamination, and blending with other fuels. Not only does the chemical composition of each fuel differ, but the composition of any particular fuel can also change with time. It is usually the formation of insoluble reaction

Manuscript approved December 29, 2005.

products or changes in a critical property that bring fuel stability into question. Very often, the chemical processes leading to stability problems are due to the presence or absence of constituents at trace concentration levels.

Considering the complexity and variability of fuels, it is not surprising that success has often eluded researchers in their efforts to understand and provide practical solutions to operational problems attributed to undesirable fuel chemistry. As a consequence, research in fuel science has tended to be inductive in nature. Unfortunately, the methodologies adopted have all too often focused on producing and quantifying insoluble reaction products, since they are the most easily quantifiable manifestation of chemical reactivity in fuel. The majority of laboratory test methods to predict the tendency of fuels to undergo deleterious changes during storage or under thermal stress are based on the assumption that all the reaction rates in a complex mixture will always double in a synchronized fashion for each 10°C increase in temperature. The Ahrennius law has thus been often employed to produce detectable quantities of insoluble products in laboratory testing within practical time periods. While the Arrhenius law is applicable for pure and simple systems, reliance on thermal acceleration of deposition from a complex mixture, such as a fuel, can often yield irrelevant results. The multiplicity of sequential and parallel reaction pathways that become available as different activation energy requirements are met at different temperatures can permit chemical processes to occur that are not necessarily possible under conditions of use. Thus, while the repeatability of many laboratory fuel test devices and methodologies can be very good, in many instances the relevance to actual conditions of use is very limited, if not absent. Therefore, it's not always realistic to attach any mechanistic significance to quantities of insoluble products formed in order to define relationships between composition and liquid-phase chemistry.

While there are limits placed on certain fuel constituents, a fuel's quality and suitability for use is based on a series of physical and chemical measurements. These measurements are performed in accordance with accepted test procedures contained in the applicable ASTM test methods[1]. The NATOPS Aircraft Refueling Manual[2] requires that aviation fuel (JP-5) received by ships for aircraft fueling, be tested for API gravity, flash point, particulates, fuel system icing inhibitor (FSII), and free water. During flight operations, the fuel that is dispensed to aircraft must be tested each day for appearance, particulates, free water and FSII. All of these tests are performed in the shipboard QA fuel laboratory, which requires significant manpower and time. The necessity of sampling and transporting fuel samples from the source to the fuel lab also entails manpower costs and safety considerations. In addition, the ASTM tests that are employed require that the analyst be trained and familiarized with the fuel test methods.

Shipboard and land-based fuel handling operations would both greatly benefit from an instrumental method to monitor fuel quality and to perform the necessary quality assurance testing. While realizing significant savings in manpower and cost, this capability would also reduce the time necessary to determine fuel quality. A sensor-based fuel diagnostics capability would significantly reduce, if not eliminate the safety and disposal issues associated with laboratory consumables now in place. If this technology could be developed to include in-line real time quality monitoring, this would be invaluable in performing fuel quality monitoring throughout the fuel handling system. Such a system could be automated to provide continuous

[1] ASTM, Specification of Aviation Turbine Fuels. *In Annual Book of ASTM Standards*; ASTM: Philadelphia, PA, 1997; Vol. 05.01, D1655-96c.

[2] "Aircraft Refueling NATOPS Manual", NAVAIR Report No. 00-80T-109, 15 Jun 2002.

real-time fuel quality monitoring for both shipboard and land-based fuel handling and distribution operations.

A sensor-based fuel quality assessment technology would rely on predictive models based on mathematical relationships between fuel composition and stability. The science of chemometrics has grown from a need to identify hidden relationships in complex data. Chemometric modeling offers the potential for rapid analysis, simultaneous prediction of multiple properties, and the ability to address large data sets automatically. Moreover, this approach would not necessarily entail stressing or other treatments that could change the chemistry. Recent advances in analytical techniques, computer technology and the science of chemometrics have made it possible to bring these technologies together to address the task of developing a useful predicative model correlating fuel stability with fuel composition.

Since the compositional features that can influence critical fuel properties are typically obscured by an abundance of irrelevant information, some of the techniques of chemometrics would seem well suited to reveal hidden information in complex data from fuel compositional analysis. Several research groups have successfully employed chemometric methods to discriminate between different fuel types from GC analyses. In 1979, Clark and Jurs[3] described automated classification algorithms that successfully characterized GC data from crude oil samples according to their origin. Neural networks have also been employed[4] to develop multivariate pattern recognition models for classifying jet fuel samples by type (e.g., JP-4 vs. JP-5). Lavine and coworkers[5] noted that mathematical pattern recognition methods offer a better approach to GC fuel analysis than visual inspection due to the complex nature of processed fuel samples. They demonstrated that pattern recognition methods could successfully identify fingerprint patterns in the GC data that were characteristic of fuel type, even in the presence of severe weathering. In each of these applications, the information needed to discriminate the fuel samples consisted of subtle variations in peak intensities distributed across multiple peaks in the chromatograms. In order to improve the selectivity and predictive power of principal component analysis of GC data, Johnson and Synovec[6] employed analysis of variance (ANOVA) calculations to restrict the analysis to only those features in the data that were relevant to the classification. In this manner, they were able to discriminate between JP-5, JP-8 and JP-TS in mixtures with as little as 1% variation in volume, using comprehensive two dimensional GC (GC-GC), and eliminate the impact of geographical variances in the jet fuel samples.

Historically, spectroscopic characterization of fuels has been a mainstay of fuels research for over 60 years, and the past 15 years have seen a surge of research focused on the development of rigorous calibration models that correlate the compositional information contained within spectroscopic data to selected fuel quality parameters. Spectroscopic methods offer a number of advantages, including the relative simplicity of instrumentation, rapid analysis time, and high quality of the data from a chemometric perspective. Chemometric multivariate analysis of spectroscopic data is desirable due to several reasons. Chief among them is the so called first order advantage, providing the ability to recognize the presence of interferants and calibrate in the presence of known interferants, as well as conferring the advantages normally provided by signal averaging. Not to be ignored, however, are the additional potentials of rapid analysis,

[3] Clark, H. A.; Jurs, P. C. *Anal. Chem.* **1979**, *51*, 616-623.
[4] Long, J. R.; Mayfield, H. T.; Henley, M. V.; Kromann, P. R. *Anal. Chem.*, **1991**, *63*, 1256-1261.
[5] Lavine, B. K.; Mayfield, H. T.; Kromann, P. R.; Faruque, A. *Anal. Chem.*, **1995**, *67*, 2846-3852.
[6] Johnson, K. J.; Synovec, R. E. *J. Chemometrics and Intell. Lab. Systems*, **2002**, *60*, 225.

simultaneous prediction of multiple properties, and the ability to address large data sets automatically.

A wide variety of fuel types, ranging from gasoline to jet and diesel, have been examined using both near infrared[7,8,9,10] and Fourier transform infrared[11] instruments as well as FT-Raman[12,13,14] instruments. A number of fuel properties have thus been predicted via chemometric regression of spectroscopic data, including octane/cetane number[15], flash point, freeze point, density, viscosity, sulfur content[16], oxygenates (such as MTBE and ethanol), aromatic, olefin, and saturate content, distillation fractions, and vapor pressure. Of these, the correlation of octane number to NIR spectra has been the most widespread and extensively developed with training sets numbering in the thousands, resulting in numerous commercially available octane analyzers.

Critical Properties	
	Flash point
	Fuel system icing inhibitor concentration
	Dirt (particulate) content
	Water content
	Density
Desirable Properties	
	Aromatics (di-aromatics and mono-aromatics
	Additives (Betz, SDA, corrosion inhibitors)
	Freeze / cloud point
	Sulfur content
	Viscosity
	Lubricity

Table 1. Fuel properties to be targeted for prediction by fuel quality sensors.

[7] Swarin, S. J.; Drumm, C. A. "Prediction of Gasoline Properties with Near-Infrared Spectroscopy and Chemometrics." SAE Paper No. 912390, 1991.
[8] Fodor, G. E.; Kohl, K. B. *Energy & Fuels*, **1993**, *7*, 598-601.
[9] Westbrook, S. R. "Army Use of Near-Infrared Spectroscopy to Estimate Selected Properties of Compression Ignition Fuels." SAE Paper No. 930734, 1993.
[10] Macho, S.; Larrechi, M. S. *Trends in Analytical Chemistry*, **2002**, *21*(12), 799-806.
[11] Gomez-Carracedo, M. P.; Andrade, J. M.; Calvino, M.; Fernandez, E.; Prada, D.; Muniategui, S. *Fuel*, **2003**, *82*(10), 1211-1218.
[12] Flecher, P. E.; Welch, W. T.; Albin, S.; Cooper, J. B. *Spectrochimica Acta*, Part A: Molecular and Biomolecular Spectroscopy, **1997**, *53A*(2), 199-206.
[13] Workman, J. Jr. *Journal of Near Infrared Spectroscopy* (review article), **1996**, *4*(1-4), 69-74.
[14] de Bakker, C. J.; Fredericks, P. M. *Applied Spectroscopy,* **1995**, *49*(12), 1766-71.
[15] Kelly, Jeffrey J.; Barlow, Clyde H.; Jinguji, Thomas M.; Callis, James B. *Anal. Chem.,* **1989**, *61*, 313-320.
[16] Breitkreitz, Marcia C.; Raimundo, Ivo M., Jr.; Rohwedder, Jarbas J. R.; Pasquini, Celio; Dantas Filho, Heronides A.; Jose, Gledson E.; Araujo, Mario C. U. *Analyst,* **2003**, *128*(9), 1204-1207.

In order to assure adequate fuel quality, the shipboard fuel laboratory must be capable of measuring the fuel properties shown in Table 1. Moreover, any new technologies put in place to accomplish this must be capable of measuring those properties with the same or better precision than current methods. The findings of an extensive survey conducted in FY04, indicated that there were no suitable commercially available solutions to measure these properties, with the possible exception of an optical light scattering sensor for the simultaneous estimation of water and particulates that is being developed by Pressure Systems, Inc. (PSI), and currently under evaluation by NAVAIR. In the first phase of this study, methodologies for chemometric modeling of chromatographic data were developed to perform sensitive and compound-specific fuel diagnostics via GC and GC-MS of Navy mobility fuels. In the second phase of this study, these methodologies were extended to fuel property modeling with both chromatographic and spectroscopic fuel analysis data. The initial emphasis was placed on determining the suitability of these various analytical tools to measure the critical fuel properties in Table 1, for implementation in a sensor-based analytical system.

3.0 FUEL DIAGNOSTIC AND PROGNOSTIC MODELING

3.1 Prediction Of Fuel Failures In A Jet Engine Combustor

An example of the discontinuity that can exist between laboratory testing and actual engine use was provided during several incidents where a jet engine combustor underwent catastrophic failure when using JP-5 fuel from a particular source. In this instance, the fuel that caused these failures passed all the standard laboratory tests required by the military specification MIL-T-5624. In addition, a suite of non-standard tests was also conducted without providing an answer to the fuel dependent engine problem. Chemical analyses did not reveal the presence of abnormal or highly reactive constituents that could have been identified as responsible for these failures. It became apparent that the compositional uniqueness of this fuel responsible for the combustor failures was too subtle to be revealed by a straightforward analytical search for known constituents. This study was therefore undertaken in order to determine if it would be possible to develop a correlation model that could predict the incidence of combustor failure, with reasonable accuracy, from a capillary GC analysis performed on the suspect fuel sample. This would provide the means to avoid costly full-scale combustion rig testing to ensure fuel suitability for this particular jet engine.

Experimental

The training set (fuel set #1) was comprised of 15 JP-5 fuels that were obtained from various sources, and verified to be in accordance with MIL-DTL-5624T. The origin of most of the samples could be traced back to one particular refinery, where the failed fuels were produced. Some samples, as shown in Table 2, were obtained from the distribution system and some from the refinery after process changes were implemented in an effort to avoid the engine failures. Samples #2 and #11 were obtained from a different refinery, and sample #14 was taken from a long-term storage facility. Fuel sample #8 was also obtained from the distribution system, but was of uncertain origin. All the samples in the training set had been tested in a full-scale jet engine combustion rig, which is a pass/fail test for combustor coking. Test samples 1, 3, 12 and 14 had failed the full-scale combustion test, while all the other samples had passed. A second group of 10 JP-5 fuels (Fuel Set #2), was obtained from a distribution system that contained fuel

from refinery #1. These samples were analyzed and classified with the model developed from the training set, (fuel set #1), prior to combustion testing.

Five replicate chromatograms were obtained with an Agilent 5890 capillary gas chromatograph, with electronic pressure control, controlled via an HP Chemstation. Samples were manually injected with a split/splitless injector at 250 °C, with a ratio of 60:1. A 50 m OV-101 (crosslinked polysiloxane) column with a flame ionization detector was used. A column heating profile was used with an initial oven temperature of 40 °C, with a heating rate of 10 °C /min, to 220 °C held for 2 minutes, giving a total run time of 20 minutes. The GC detector current was sampled at a rate of 20 Hz, giving a resolution of 50 ms per point.

A measured quantity of n-eicosine (n-C_{20}) was added to each sample as an internal standard to compensate for variations in sample injection and detector response. The positions of the GC peaks in all the samples were aligned to match the retention time of the internal standard in one reference chromatogram. Peak heights were also normalized using the internal standard peak from the same reference sample. Before beginning data analysis, the original chromatographic data set of 75 chromatograms and 16384 data points was reduced in size in order to make it more manageable by computer. Every eighth data point in the chromatograms was used to create a reduced data set (75 x 2048), which represented a chromatographic sampling frequency of 2.5 samples per second (compared to 20 samples per second with the original data). The data were reorganized so that replicate chromatograms were ordered consecutively.

Sample No.	Combuster Test Pass / Fail	Fuel Source
1	Fail	Refinery #1, from distribution system
2	Pass	Refinery #2
3	Fail	Refinery #1, from distribution system
4	Pass	Refinery #1, process varied, sampled at refinery
5	Pass	Refinery #1, process varied, sampled at refinery
6	Pass	Refinery #1, from distribution system
7	Pass	Refinery #1, from distribution system
8	Pass	Unknown source, from distribution system
9	Pass	Refinery #1, process varied, sampled at refinery
10	Pass	Refinery #1, process varied, sampled at refinery
11	Pass	Refinery #3, sampled at refinery
12	Fail	Refinery #1, sampled at refinery
13	Pass	Refinery #1, from distribution system
14	Fail	Sampled from long-term storage facility
15	Pass	Refinery #1, process varied, sampled at refinery

Table 2. Description of JP-5 fuels used to develop the correlation model (fuel set#1).

Results and Discussion

In order to investigate the similarities in the fuel samples, a non-linear map of the data is shown in Figure 1. Non-linear mapping provides a visual means of displaying the multidimensional chromatographic data in two dimensions by preserving the inter-chromatogram distances. In interpreting this plot, the distances between the chromatograms is a measure of their mathematical similarity (e.g., Euclidean distance). Thus, two chromatograms located near each other in a non-linear map have similar chromatographic profiles. Ideally, one would like to see the replicates of the same samples clustered together and the samples from the two classes of fuels ordered into distinct groups. In this plot, the engine failing samples are 1, 3, 12 and 14; and all others are engine passing. Figure 1 clearly shows that samples 8 and 11 are different from the other samples, due to the tight clustering away from the other samples. The lack of distinct clustering between the engine passing and failing classes suggests that the differences between the classes are minor. The small distances between the engine passing samples and failing samples 3 and 12 shows that these two samples are more similar to the passing samples than the other failing samples 1 and 14.

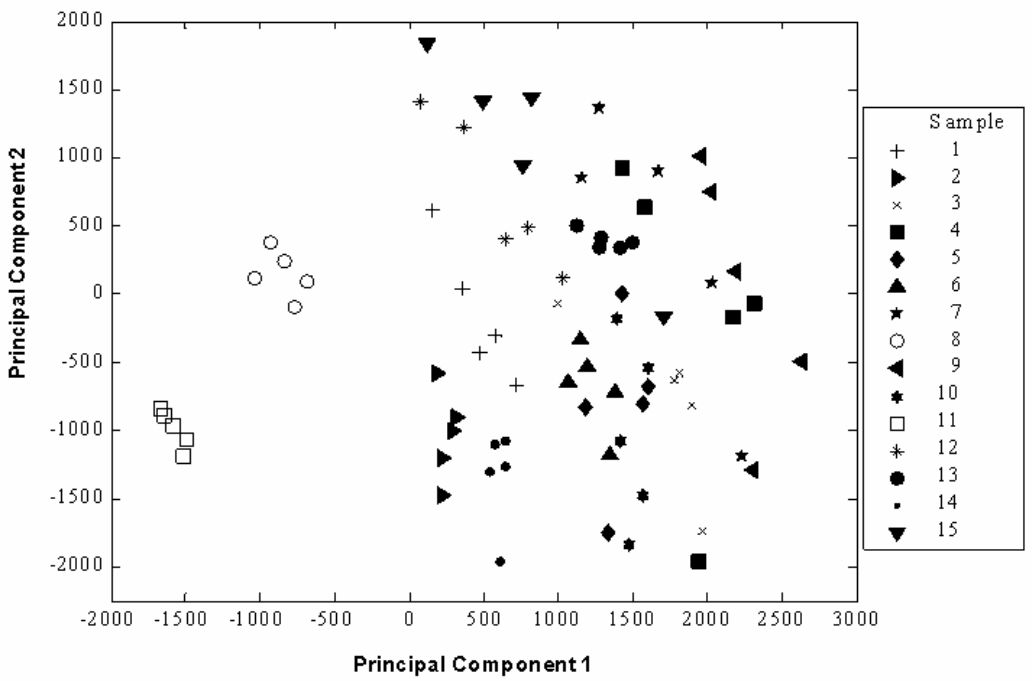

Figure 1: Non-linear map of chromatographic data from 15 different jet fuel samples. Samples 1, 3, 12 and 14 caused engine failures.

Due to the placement of the samples 8 and 11 in the nonlinear map further outlier analysis was warranted. Principal components analysis (PCA) is a multivariate data reduction method that provides both a useful visualization tool and a statistical baseline for outlier analysis. PCA finds combinations of variables, or factors, that describe major trends in the data. In interpreting this plot, the distances between the points is a measure of their similarity. Thus, two points located near each other in a PCA plot would be expected to have similar chromatographic information. Ideally, replicates of the same sample would be clustered together and the samples from the two

classes of fuels (pass or fail) would be ordered into distinct groups. Figure 2 is a plot of the 75 chromatograms projected onto their first two PCs. Overlaid on the PCA plot is the 99% confidence interval for the PC scores. The five chromatograms that lie outside of this sphere all come from sample 11.

Since one of the goals of this project is to develop a single classification model that can discriminate good fuels from bad fuels, regardless of the source, subsequent analysis was performed using data sets with and without sample #11. The decision to remove an outlier from model development is non-trivial, and it is advisable to include as many samples as possible, particularly in this case, where samples were limited. However, severe outliers such as sample #11 can skew the PCA model such that the small differences necessary for distinguishing between passing and failing samples would be masked. Potential causes for outliers might be samples taken from different sources, jet fuel types (e.g., JP-8), or major changes in the instrumental response. Upon visual inspection of the chromatogram, it is clear that the GC of fuel #11 was distinctly different than the other fuels in the data set. Fuel #11 was the only fuel obtained from refinery #3, and was correctly identified as an outlier in the analysis. Thus, the amount of variation between this fuel and the other fuels was much greater than the differences between the fuels from the same source.

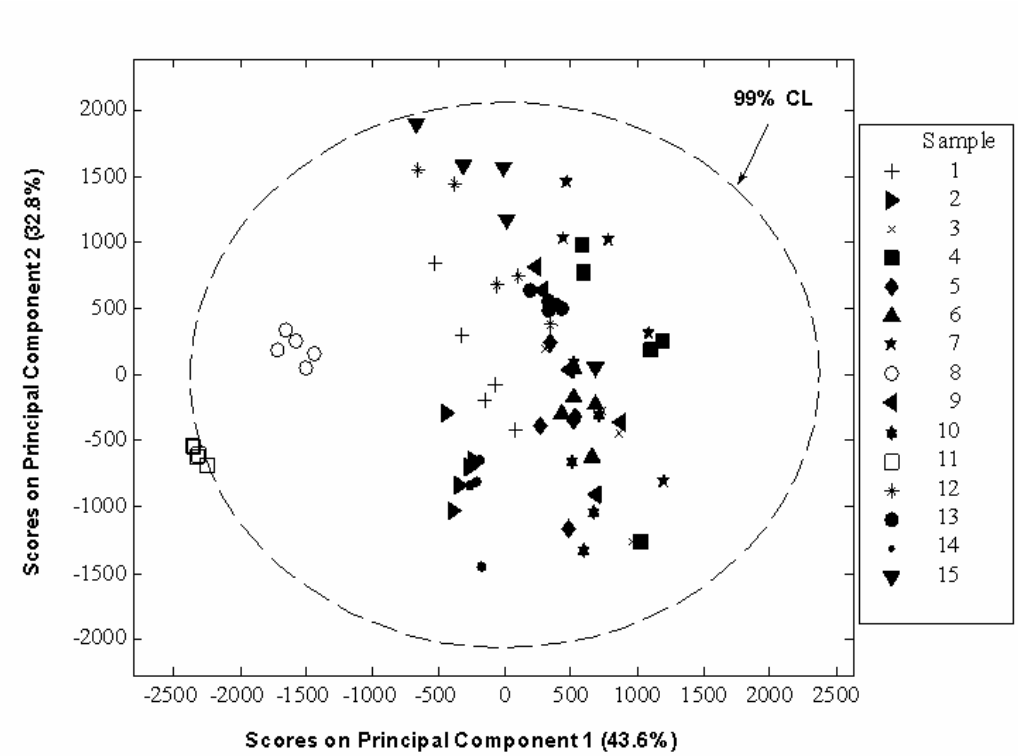

Figure 2: Principle component analysis of chromatographic data from 15 jet fuel samples.

Discriminant partial-least-squares regression (DPLS) was used to classify the sample chromatograms as belonging to either engine passing or failing fuel samples. DPLS uses a linear approach for classification, and the model is of the form

$$\hat{c}_i = b_0 + b_1 x_{i,1} + b_2 x_{i,2} + \ldots + b_n x_{i,n} \quad (1)$$

where $\hat{c}_i$ is the predicted class for sample i, the b terms are the multivariate regression coefficients, and the x_i terms are the detector responses for the $i = 1$ to n data points ($n = 2048$).[17] Two different prediction models were constructed; data set 1 contained the outlier fuel #11, and this fuel outlier was removed from data set 2, and two methods of model validation were employed. Since multivariate calibration methods are prone to over fitting the data, they must be properly validated. Ideally, validation of the model would be done with an external prediction set consisting of data withheld from the data used to develop the model, i.e., the training set. However, in this instance, samples were at a premium and internal validation methods such as cross-validation were used. The first validation method, leave-one-out cross-validation, involves removing one chromatogram from the data set and predicting its fuel class based on the remaining 74 or 69 chromatograms, for data sets 1 and 2, respectively. This is repeated until each of the chromatograms has been removed and predicted once. The second validation method, contiguous blocks cross-validation, involves removing all five of the replicate chromatograms for one sample from the data set and using the remaining chromatograms to predict the class of the five removed. This is repeated until each of the samples has been removed from the data set and predicted once. The contiguous blocks cross-validation method is a more rigorous method since it predicts the samples versus the other 14 samples. In comparison, leave-one-out predicts each chromatogram against the other 14 samples and 4 replicates of the same sample. Typically, the leave-one-out cross-validation can easily over-estimate the classification ability of the model when a large number of replicates and a small number of samples exist. The optimal number of latent variables or PLS factors was chosen to be the minimum predicted residuals sum of squares (PRESS) statistic using contiguous blocks cross-validation. This allows for enough information to be retained to explain the model, but not overfit the specific data in the training set.

A third data set was prepared by performing a systematic search of the chromatographic data in order to find specific retention time windows that have discrimination power superior to the full chromatogram. This method, known as interval-partial least squares regression (i-PLS), was performed on data set 2. i-PLS determined that the optimum data range for discrimination was between data channels 392 and 683, resulting in a 75×292 data matrix. The location of this chromatographic window in relation to the full chromatogram is shown in Figure 3. The DPLS classification results are given in Table 3. In the Table, methods *l-o-o* and *contiguous* represent leave-one-out cross-validation and contiguous blocks cross-validation, respectively. The Table shows that all the samples are classified correctly using leave-one-out cross-validation, except for two replicate chromatograms for sample 6 being incorrectly classified with data set 3. However, as noted above the contiguous blocks cross-validation is a considerably more robust validation.

The results for data set 1 show that the classification performance is poor with only 62.6% of the samples being classified correctly. The essentially unchanged results for data set 2 shows that the removal of outlier sample 11 does not affect the performance of the classification model. Significant improvements in classification performance were obtained with data set 3. These improvements suggest that the subtle differences in the chromatographic profiles in this retention time window may correlate with a fuels performance in the engine test. The results for data set 3, with contiguous blocks cross-validation are also shown in Figure 4. This Figure shows the predicted class output $\hat{c}$ for each of the samples, except for sample 11. In this Figure, a $\hat{c}$ value of greater than zero represents a predicted engine passing fuel and a $\hat{c}$ of less than zero represents a

[17] Thomas, E. V. *Anal. Chem.*, **1992**, *66*, 795A-804A.

predicted engine failing fuel. Three engine failing sample chromatograms, belonging to fuel samples 3 and 12 rise above the line $\hat{c} = 0$, and are hence misclassified as engine passing fuels. Four engine passing sample chromatograms, from fuel samples 2 and 6, fall below the line $\hat{c} = 0$, and are misclassified.

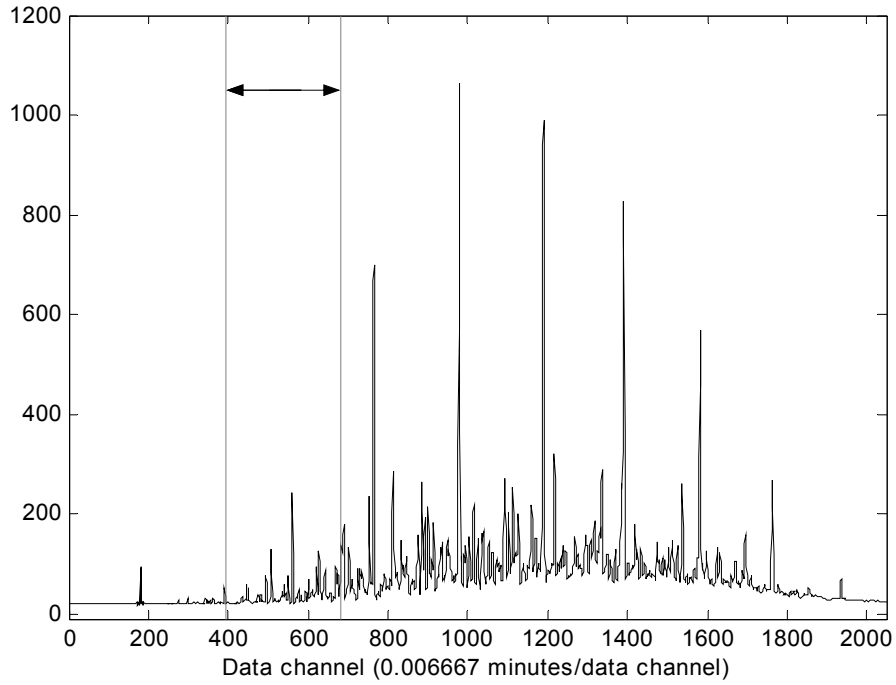

Figure 3. Range of data channels picked by interval-PLS. (2.61 to 4.55 minutes)

Data Set	Method	Class: Pass correct/n (%)	Class: Fail correct/n (%)	Overall % correct
1	l-o-o	55/55 (100)	20/20 (100)	100
2	l-o-o	50/50 (100)	20/20 (100)	100
3	l-o-o	48/50 (96)	20/20 (100)	97.14
1	contiguous	41/55 (74.5)	6/20 (30)	62.6
2	contiguous	37/50 (74)	6/20 (30)	61.4
3	contiguous	46/50 (92)	17/20 (85)	90
4	DS3	44/50 (88)	NA	88

Table 3. DPLS predictions by the model for the training sample set, using two methods of validation. Data set #1 is all the fuel samples, and data set #2, with the outlier fuel #11, removed.

A blind prediction test was performed on a distinctly different group of fuels (data set #4), gas chromatographic data from a set of ten blind fuel samples, were analyzed by DPLS to further validate the model performance. Five replicate chromatograms were received for each sample. The chromatograms were reduced in size to the same region chosen by the i-PLS model resulting in a 50×292 data matrix. A new DPLS model was built using all 14 samples from data set #3. As shown in Figure 5, the DPLS model classified one replicate from six of the ten fuel samples as failing, with the remaining 44 of the 50 samples analyses as passing (88%). Subsequent combustion testing classified all the samples in data set #4 as passing.

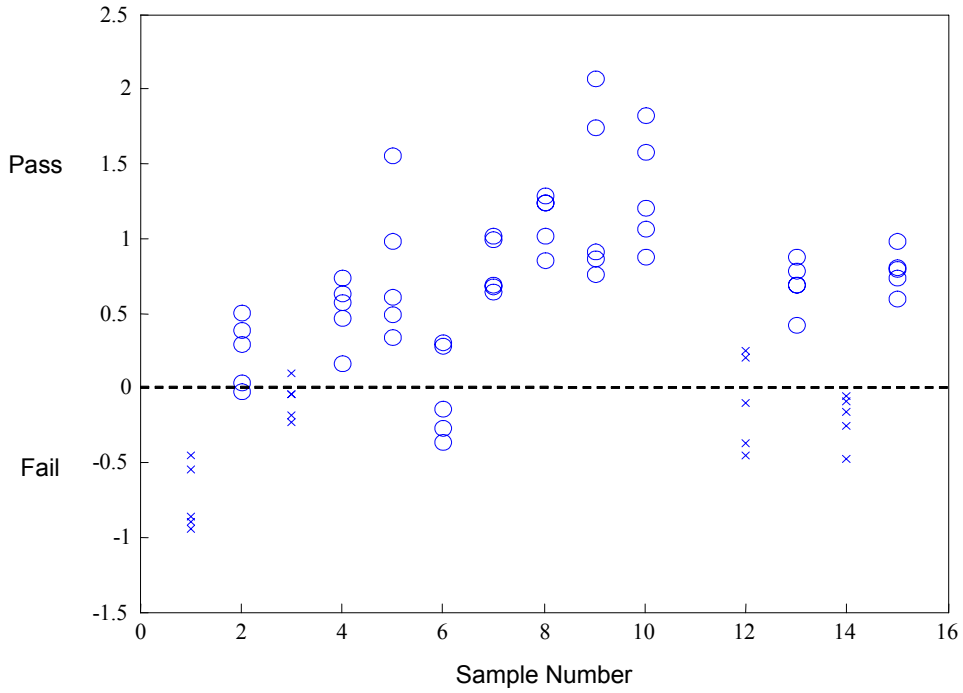

Figure 4. DPLS cross-validation results from data set #3, contiguous blocks method

Summary of Results

The results of this preliminary study illustrate how, with proper preprocessing methods, fuels can be classified with respect to performance on the basis of subtle differences in fuel constituency. The findings also illustrate the impact that relatively minor variations in GC operating conditions can exert on multivariate correlations when the analysis is focused on the minor differences between samples. While it is important to consider all the data, proper preprocessing of the raw data is essential in order to focus the analysis on the differences between the samples without undue interference from those fuel constituents common to all fuels and to minimize instrumental variations so that the method can be packaged and used with any suitable instrumentation. It was also shown that the discriminating power of the model could be improved by focusing on those portions of the data that have greater statistical weight, thus reducing the amount of extraneous information in the data set.

In this study, there were a limited number of failed fuels available, and the levels of uncertainty reached in the validation samples reflect this. These variations would be significantly lower if the number of available failed fuels were greater. However, using the preliminary model developed with this data, we were able to correctly screen a group of fuels that passed the combustor test, with very little uncertainty.

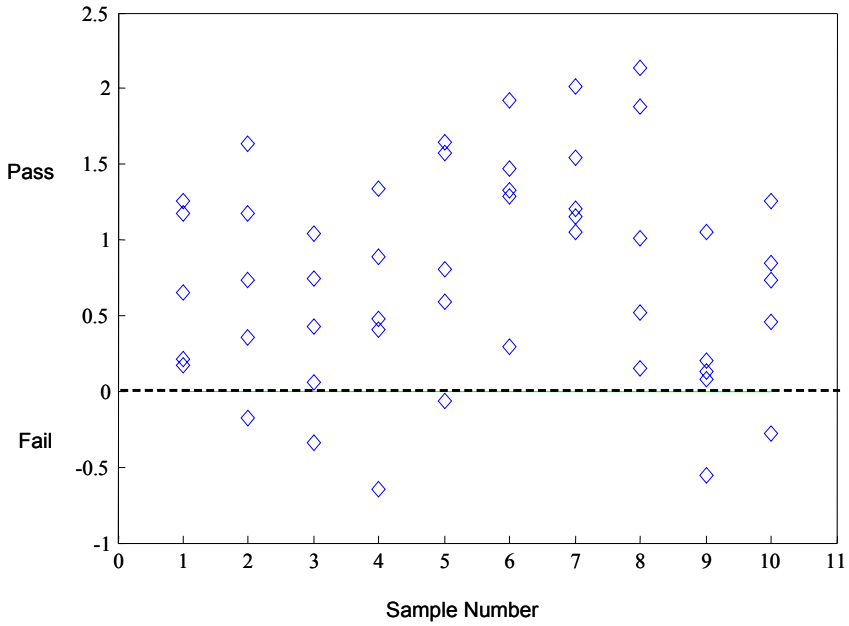

Figure 5. DPLS prediction results from jet fuel data set #2.

While chemometrics can be successfully employed to discriminate between different fuel types or sources, there are practical limits on use of gas chromatography with fuels that have substantially different compositions. In order to develop useful correlations between composition and performance with multivariate analysis of fuels from widely distributed sources and crude slates, the methods developed in this study could be focused, through interval analyses, on the compounds of interest. For example, if a particular compound class was identified as being significant, the fuel could be preprocessed and a model developed for the subset of all fuel constituents represented by that compound class. However, chemical changes that can lead to undesirable fuel property changes are generally due to the presence of chemically active fuel constituents, such as heteroatomic species and transition metal chelates. Thus, while GC with flame ionization detection would not necessarily respond directly to metal compounds and perhaps some heteroatomic species, their impact on hydrocarbon constituency would be detected by this method, if the magnitude of the changes were within detection limits.

3.2 Monitoring Diesel Fuel Degradation by GC-MS and Chemometric Analysis

This study was undertaken in order to determine if the application of multi-way chemometric techniques to a 3-dimensional dataset, such as GC-MS, would overcome the limitations of GC alone in characterizing minute chemical changes in fuels, regardless of source.

Experimental

Fuel Stressing. A specification naval distillate fuel (NATO F-76) fuel was used for these studies. In storage stability testing by the LPR method in accordance[18] with ASTM D5304, this fuel produced 0.7 mg sediment per 100 mL. Two methods of thermally stressing the fuel were used in order to provide fuel samples with varying levels of thermal degradation for analysis by GC-MS. In the first study, 100 mL of fuel was placed in a vented 250 mL borosilicate glass bottle and stored in an oven, in the dark at 60 °C. Aliquots (1 mL) were periodically withdrawn without cooling for GC-MS analysis at 0, 7, 14, 24, 31, and 37 days of oven stress. In a second study, fuels were subjected to stress in a closed, low pressure reactor (LPR). LPR stress was performed on aliquots of fuel in accordance with ASTM D5304 (i.e., at a temperature of 100 °C and under an atmosphere of 100 psig oxygen) for both the standard duration of 16 hours and also an extended duration of 42 hours. The extended duration LPR conditions were chosen to guarantee significant oxidative changes in the fuel. After the fuel samples were removed from the LPR, they were cooled in the dark and 2 mL aliquots were filtered through a 0.2 μm nylon Millipore filter for analysis. A summary of the LPR-stressed samples analyzed by GC-MS is presented in Table 4.

GC-MS Analysis. GC-MS data were obtained using an HP 5890 Series II gas chromatograph coupled to an HP 5971 mass selective detector. Replicate dilutions were prepared and analyzed for each fuel sample: three replicates per oven-stressed sample and six replicates per LPR-stressed sample. Each replicate was prepared by dissolving 7.5 μL of fuel in 1500 μL dichloromethane. An HP 6890 injector and autosampler delivered 1.0 μL aliquots of each replicate sample to the GC in a random order. A split/splitless injector at 250 ^{o}C with a split flow ratio of 60:1 was used along with a 50 m x 0.2 mm Agilent HP-1 (dimethylpolysiloxane) capillary column. The oven temperature profile was 60 ^{o}C to 288 ^{o}C at 3 ^{o}C/min, giving a run time of 76 minutes. A solvent delay of 4.40 minutes was used which reduced the data acquisition time to 71.6 minutes per run.

Chemometric Analysis. Following acquisition, GC-MS chromatograms were preprocessed to minimize any undesired variation between chromatograms. First, all chromatograms were normalized to unit area to minimize effects due to variation in injected sample volume. Next, the chromatograms were retention time aligned in order to minimize retention time variation between chromatograms due to unavoidable fluctuations in instrument parameters (e.g. oven temperature, flow rate, etc.) during the course of the experiments.

---

[18] ASTM, "Standard Test Method for Assessing Middle Distillate Fuel Storage Stability by Oxygen Overpressure". In Annual Book of ASTM Standards; ASTM: Philadelphia, **2003**; Vol. 05.03, ASTM D 5304-03.

Sample Number	Stress Conditions
1-6	Unstressed
7-11	LPR, 16 hour
12-17	LPR, 42 hour
18-23	LPR, 42 hour, Cu

Table 4. Summary of fuel stress conditions imposed on the 23 samples of naval distillate fuel (NATO F-76).

Retention time alignment for these experiments was accomplished via a two-step procedure. First, a total ion current (TIC) chromatogram for each GC-MS chromatogram was constructed by taking the sum along the mass spectral axis in the data. The set of all TIC chromatograms was then subjected to a manual peak alignment procedure where corresponding peaks from chromatogram to chromatogram were visually identified and tabulated. Taking the first chromatogram as the target for alignment, the required shifts for the remaining chromatograms were calculated. In the second step, these required shifts were applied to the retention time axis of the GC-MS chromatograms via interpolation.

Since the data acquired for this work were accumulated over a relatively short time period on a single instrument, the instrumental parameters could be more closely controlled than is generally possible in daily routine analyses. Given the relative stability of the GC-MS data acquired, it was unnecessary to add internal standards for retention time alignment and normalization purposes in this experiment. In general practice under conditions where carrier gas flow rate variations are encountered, it certainly may be necessary to employ internal standards. In previous studies[19], we have successfully corrected non-linear variations in gas chromatography carrier gas flow rates by aligning chromatograms within portions of the data bracketed by the major hydrocarbon peaks. Such a windowed approach to baseline peak alignment is a viable approach to minimizing instrumental variations that could be encountered in actual use and when the best possible quantitative precision is required.

Datasets for each experiment consisted of a series of two-dimensional GC-MS chromatograms, one for each sample analyzed, stacked on each other to form a three-dimensional array, or cube of data. These data sets were probed for chromatographic features that described the difference between different fuel blends using the ANOVA based feature selection algorithm as described by Johnson[20], and implemented by an in-house program written for MATLAB (Mathworks Inc., Natick, MA). Feature selection was performed by grouping a set of data into defined classes and looking for data points which best describe the differences between classes, while remaining the same within a given class. This is accomplished by performing the ANOVA f-ratio calculations, shown in equations 2 – 5, for each data point in the two dimensional space of the GC-MS data. In this manner, a complex data set was rapidly and automatically scanned for features important for a given classification. Multivariate models of GC-MS data were then

[19] Morris, R. E.; Hammond, M. H.; Shaffer, R. E.; Gardner, W. P.; Rose-Pehrsson, S. L. *Energy & Fuels,* **2004**, *18,* 485.
[20] Johnson, K. J.; Synovec, R. E. *Chemom. Intell. Lab. Sys.* **2002**, *60*, 225-237.

constructed to describe compositional differences between fuel samples. Modeling was accomplished via the PLS toolbox and the Nway toolbox[21] (version 2.1). Three separate techniques were used to model changes in fuel composition, multi-way principal components analysis (MPCA), parallel factor analysis (PARAFAC), and multilinear partial least squares regression (N-PLS)[22,23,24,25].

MPCA amounts to unfolding each two dimensional chromatogram into a vector of data and subjecting the resulting set of vectors to standard PCA[26]. PCA functions by constructing a basis set of orthogonal vectors that most efficiently describe the variation present in the data set, known as loadings, and the projections of each sample onto a particular loadings vector are known as scores. Prior to application of MPCA, the GC-MS data in this work was subjected to an eight-point boxcar average along the chromatographic dimension of the data to reduce the size of the data set due to memory limitations of the personal computer on which the analysis was performed.

PARAFAC is conceptually similar to PCA, except that it functions on three-dimensional arrays. Thus, each independent factor in a PARAFAC model consists of three loadings vectors, one for each dimension of the original data set (i.e., retention time, ion abundance and mass spectra). The loadings vectors generated by PARAFAC are calculated in an iterative fashion to best describe the overall variation in the data set, given a specified number of factors as well as any constraints that may be imposed on any of the modes, such as non-negativity or unimodalitiy.

The advantage of PARAFAC lies in the incorporation of a third dimension, which provides unique solutions to the factor decomposition problem. Thus, if the underlying factors fit the PARAFAC model, concentration and spectral features can be extracted directly. According to the strength and weaknesses of each technique, bulk changes in fuel composition (i.e. changes reflected in the overall chromatogram) were modeled with MPCA due to their deviation from trilinearity, while PARAFAC was used to model smaller local regions of GC-MS data in order to extract concentration profiles and mass spectra of pure fuel components.

N-PLS[27,28,29,30] is a multi-way generalization of the commonly used partial least squares regression algorithm designed to be used with second or higher order data sets. In accordance with the philosophy behind first-order PLS regression, the algorithm seeks to decompose the data into a factor model that best describes the covariance between the dependant (predicative) and independent (predicted) variables. This model is then applied to subsequently measured data to make quantitative predictions. The chief difference between PLS and N-PLS is that, in N-PLS, the factor model is trilinear in form (as with PARAFAC). N-PLS has previously been shown[31,32]

---

[21] Andersson, C. A.; Bro, R. *Chemom. Intell. Lab. Syst.* **2000**, *52*, 1-4.
[22] Smilde, A. K. *Chemom. Intell. Lab. Sys.* **1992**, *15*, 143-157.
[23] Henrion, R. *Chemom. Intell. Lab. Sys.* **1994**, *25*, 1-23.
[24] Dahl, K. S.; Piovoso, M. J.; Kosanovich, K. A. *Chemom. Intell. Lab. Sys.* **1999**, *46*, 161-180.
[25] Bro, R. *Chemom. Intell. Lab. Sys.* **1997**, *38*, 149-171.
[26] Malinowski, E. R. "Factor Analysis in Chemistry" 2nd ed., John Wiley & Sons, New York, 1991.
[27] Bro, R. *J. Chemom.* **1996**, *10*(1) 47-61.
[28] Smilde, A. K. *J. Chemom.* **1997**, *11*(5), 367-377.
[29] de Jong, S. *J. Chemom.* **1998**, *12*, 77-81.
[30] Bro, R.; Smilde, A. K.; de Jong, S. *Chemom. Intell. Lab. Syst.* **2001**, *58*(1), 3-13.
[31] Johnson, K.J.; Prazen, B.J.; Young, D.C.; Synovec, R.E. *J. Sep. Sci.* **2004**, *27*, 410-416.

to be effective in the quantification of multi-component compositional properties of both industrial naphtha and fuel samples by GC-GC.

$$\textbf{\textit{f}-ratio} = \frac{\text{variance between different samples}}{\text{variance between replicates of single sample}} \qquad (2)$$

$$\textbf{\textit{f}-ratio} = \frac{\text{between-class variance}}{\text{within class variance}} = \left[\frac{\sigma^2_{\text{class}}}{\sigma^2_{\text{err}}}\right] \qquad (3)$$

$$\sigma^2_{\text{class}} = \frac{\sum (\bar{x}_i - \bar{x})^2 n_i}{(k-1)} \qquad (4)$$

$$\sigma^2_{\text{err}} = \frac{\left[\sum\sum (x_{ij} - \bar{x})^2\right] - \left[\sum (\bar{x}_i - \bar{x})^2 n_i\right]}{(N-k)} \qquad (5)$$

k = #classes (# samples)

$\bar{x}_i$ = mean of i^{th} class (sample)

$\bar{x}_{ij}$ = i^{th} measurement of class j

n_i = #measurements in i^{th} class

N = #GC-MS spectra

Results and Discussion

There are two basic premises for applying chemometric methods to instrumental data. The first is that the dataset constitutes an accurate numerical representation of the relevant chemical information, and the second is that the differences between the different classes of samples are statistically greater than the differences between samples within the same class. If these two criteria are met, then it should be possible to develop predictive and diagnostic models based on these numerical representations of fuel composition. Moreover, a mathematical discrimination of all the significant differences in fuel composition after stress could reveal subtle features highly correlated with fuel quality that could have gone otherwise undetected.

[32] Prazen, B.J.; Johnson, K.J.; Synovec, R.E. *Anal. Chem.* **2001**, *73*(23), 5677-5682,.

The data resulting from a single GC-MS analysis of a typical unstressed diesel fuel can be depicted in a two-dimensional plot as shown in Figure 6, which is a topographical contour plot with a single contour line drawn at a value of signal intensity of three times the baseline noise. In this Figure, the x-axis is retention time in terms of mass spectral scan number and the y-axis is the mass spectral axis and encompasses mass to charge (m/z) ratios of 50 to 300. Thus, each slice of this plot taken along the x-axis represents the mass spectrum recorded at a given retention time in the GC separation. A data set resulting from multiple GC-MS analyses can thus be conceptualized as a series of two-dimensional GC-MS chromatograms stacked one on top of another to form a cube. Therefore, in addition to dimensions describing GC retention time and MS mass to charge ratios, such a data set also has a third dimension reflecting the identity of the different samples subjected to GC-MS analysis.

An initial examination of the GC-MS data indicated that the chromatographic retention time precision and signal reproducibility were relatively high. For example, the data collected in the study of LPR-stressed fuels exhibited a mean standard deviation in peak position of 2.7 scan numbers across 286 peaks in the 18 chromatograms. This deviation is equal to only roughly one fourth of the typical peak width and, thus, manual alignment of the chromatographic profiles was readily achieved. Turning to signal reproducibility, an examination of replicate total ion current chromatograms yielded a mean RSD of 9.6 percent across the entire chromatographic run for the raw data, and a mean RSD of 3.3 percent for data that had been area normalized and aligned.

An MPCA model was constructed from data acquired in the analysis of the oven stressed neat fuel samples. The scores on the first principal component of the MPCA model are shown in Figure 7. This plot indicates that there is a clearly defined progressive change in composition as the fuel was subjected to increasing durations of oven stress at 60°C.

The loadings vector (reshaped to matrix form) associated with the first principal component of the MPCA model and represents the portions of the GC-MS data that were undergoing changes during oven stress. The loadings plot thus derived, indicated that much of this change was associated with a decrease in the concentrations of early eluting (i.e. high volatility) components, which is consistent with evaporative loss during stress, rather than chemical changes associated with fuel degradation. Models constructed from fuels spiked with copper demonstrated similar behavior.

The extent of the compositional changes associated with evaporative loss was further examined with the ANOVA based feature selection utility.[20] The f-ratios from this analysis are shown in Figure 8 as a contour plot drawn with a single contour line at an f-ratio value just above baseline noise. The variations from sample to sample shown for this data set in Figure 7 are thus dominated by decreasing concentrations of early eluting components. This finding indicates that the process of evaporative loss, rather than fuel degradation is being modeled. To further illustrate this point, a feature-selected total ion current (TIC) chromatogram was constructed by including only data points with an ANOVA f-ratio greater than 80, as shown in Figure 9. This feature-selected TIC thus represents only those fuel components that had changed during the oven test. When compared with the TIC of the unstressed fuel, two things are evident: 1) the ANOVA f-ratio test is able to detect subtle changes in composition from GC-MS data and 2) the lighter components were being lost during oven testing.

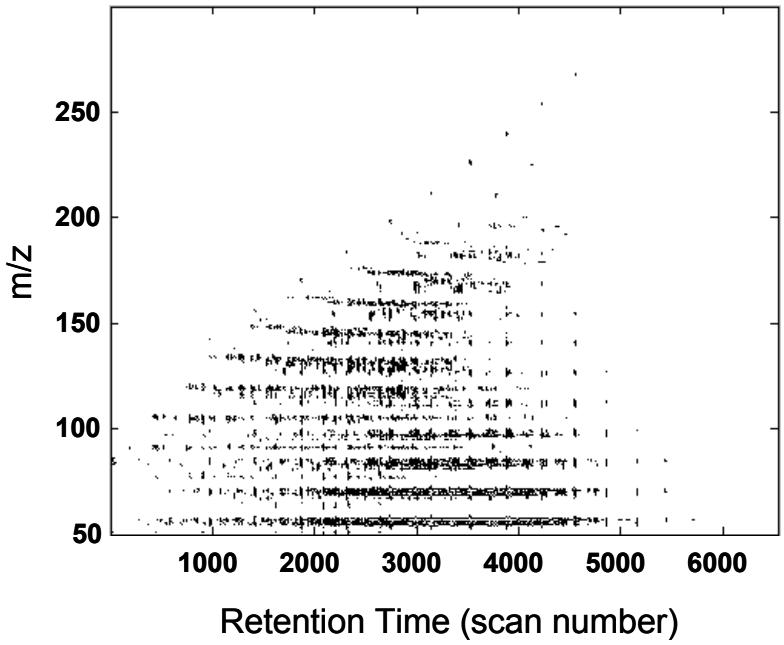

Figure 6. Typical GC-MS chromatogram of an unstressed diesel fuel, presented as a topographical contour plot with only one contour line, drawn at a signal intensity of three times the baseline noise.

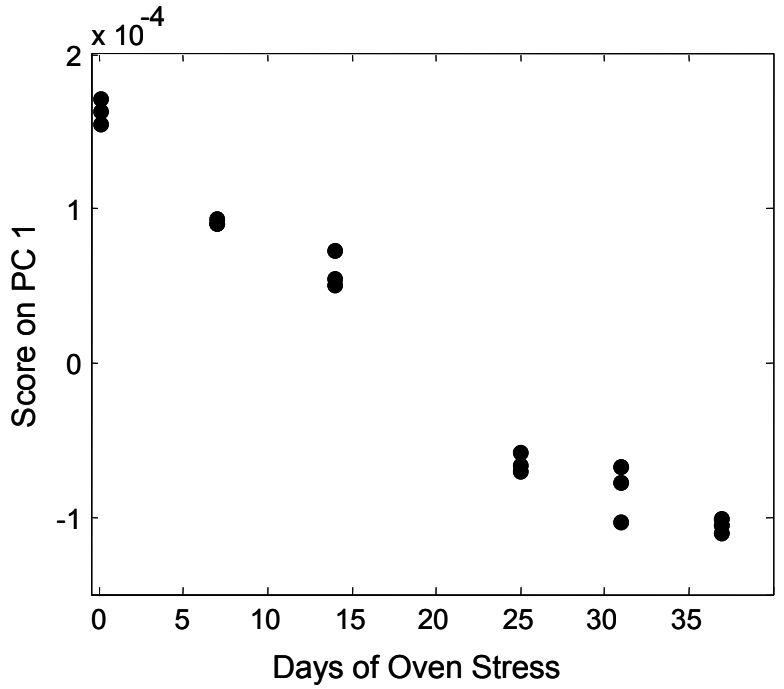

Figure 7. MPCA model of oven-stressed fuel, showing a clear progression in the scores on the first principal component as the duration of oven stress at 60°C is increased.

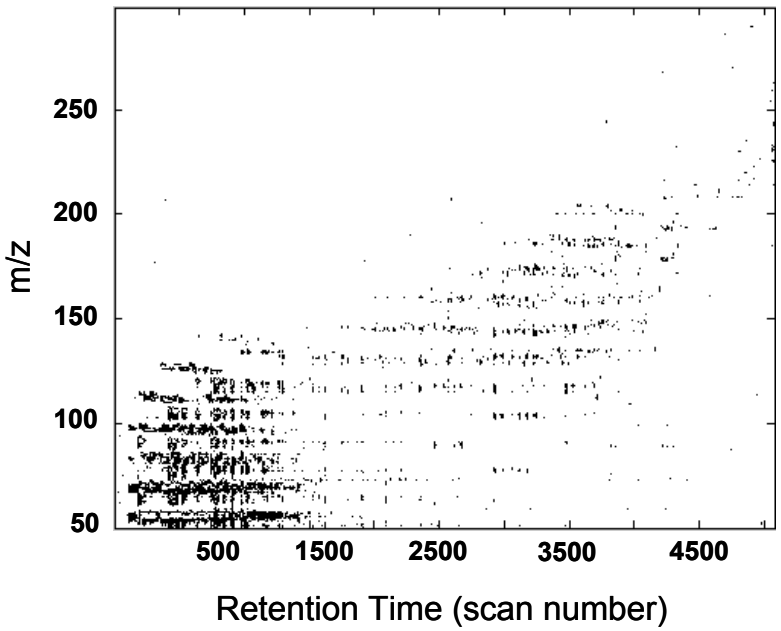

Figure 8. ANOVA f-ratios for oven-stressed fuel, which provide a measure of how well each data point describes the differences as oven stress increased.

In order to minimize evaporative losses, a second study was conducted in which neat and copper-doped fuel samples were thermally stressed in a low pressure reactor (LPR) at 100 degrees Celsius under 100 psi. oxygen for 42 hours. Figure 10 depicts ANOVA f-ratios for the LPR-stressed fuel data set. The f-ratio calculation was made by defining the classes of samples as unstressed, 16 hour LPR stressed neat, 42 hour stressed neat, and 42 hour LPR stressed with Cu, thus providing a measure of how well each data point in the GC-MS chromatograms describes the difference between LPR stressed and unstressed fuels. As can be seen in Figure 10, evaporative loss does not dominate the changes associated with LPR stress of this fuel, as they do in the first oven stress study.

An MPCA analysis of the LPR-stressed fuel data set was conducted and the scores on the first principal component are shown in Figure 11. The first six samples are replicates of unstressed fuel, the next five were 16 hour LPR-stressed fuel, the next six 42 hour LPR-stressed fuel, and the final six 42 hour LPR-stressed fuel with added copper. From this plot, there is a clear differentiation between stressed and unstressed fuels (i.e. intra-replicate variation is much less than inter-replicate variation), but essentially no difference between the comparison of stressed fuels with and without copper. The loadings from this first principal component of the MPCA model agree very closely with the features defined by the ANOVA f-ratio calculation, and this indicates that the MPCA model is describing the difference between stressed and unstressed fuels without the need for feature selection prior to MPCA. A second ANOVA f-ratio calculation

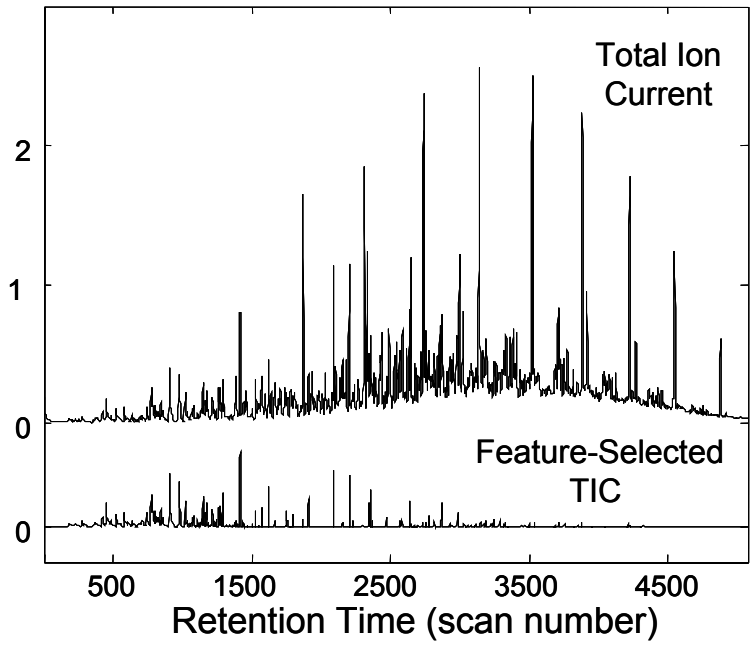

Figure 9. TIC of unstressed fuel and the feature-selected TIC of the components that have been altered during oven stress.

was performed, this time using only the 42 hour LPR-stressed fuels and defining two classes: fuels stressed with copper and fuels stressed neat. This analysis failed to locate any chromatographic features capable of making this classification. This suggests that, even though copper can accelerate the rate of fuel autoxidation, in this instance, the presence of copper had little or no significant impact on the final composition of the LPR-stressed fuel.

The feature-selected TIC displayed in Figure 12 was computed using the ANOVA f-ratios shown in Figure 10 to filter the chromatogram of an unstressed fuel so that only the chromatographic features that differ significantly between the LPR-stressed and unstressed fuels are seen. The raw (i.e. non-feature selected) TIC of the unstressed fuel is also shown, for comparison. In this instance, the feature selected TIC was calculated by including only data points with an ANOVA f-ratio greater than 100. This threshold value was chosen empirically, based on a visual inspection of all of the calculated ANOVA f-ratios, which demonstrated that ANOVA f-ratios in the baseline areas of the chromatogram were all less than 100. A more rigorous optimization of this threshold was not undertaken as the threshold obtained by visual inspection performed adequately for the purposes of this study. Figure 12B shows an enlarged region of Figure 12A and demonstrates the degree to which fuel components which changed during LPR stress were intermingled with those that did not in the GC-MS chromatogram.

An attempt was made at spectral deconvolution of an ANOVA–selected feature from GC-MS data of LPR-stressed fuel. The boxed region in Figure 12B was subjected to PARAFAC decomposition with unimodality and nonnegativity constraints on the GC mode, and nonnegativity constraint on the mass spectral mode. A five-component PARAFAC model was then constructed and the chromatographic and sample mode loadings are shown in Figure 13. As seen in Figure 13A, four discrete Gaussian peaks, as well as a fifth peak that was somewhat less well-defined, were extracted from the region shown in Figure 12B. One of this set of four peaks

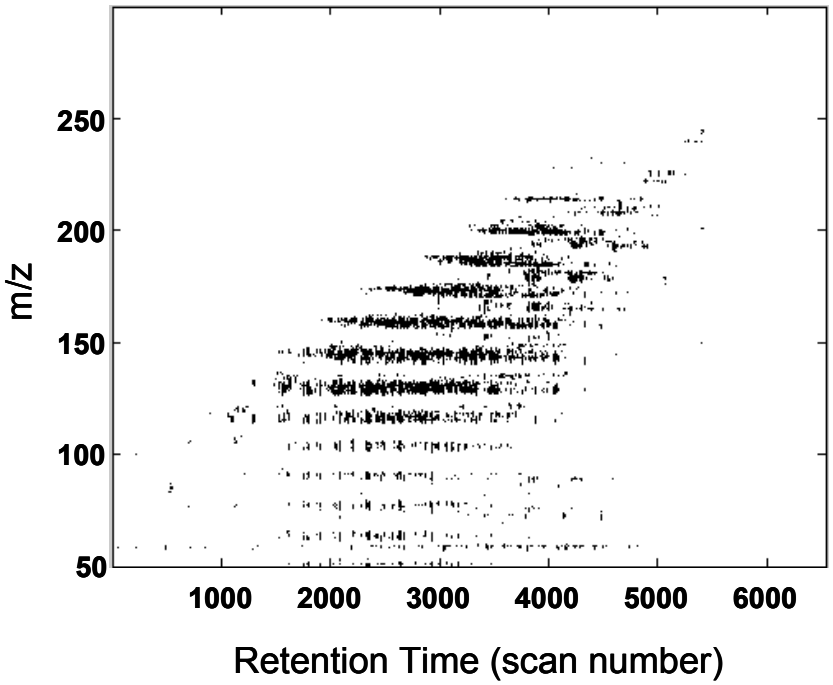

Figure 10. ANOVA f-ratios for changes in composition of LPR-stressed fuels. In this case, evaporative losses do not dominate the changes associated with LPR stress, as they do with oven stress.

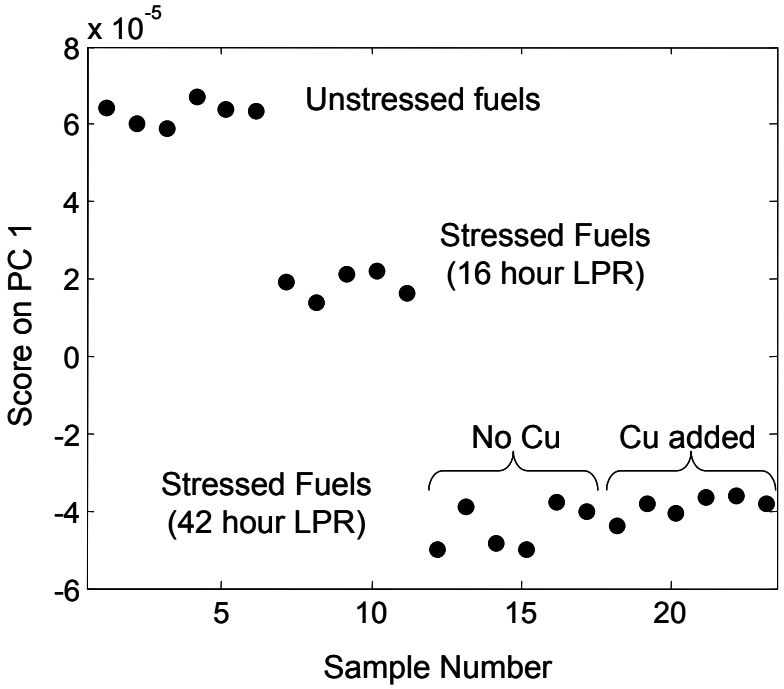

Figure 11. MPCA scores on the first principal component of LPR-stressed fuel showing a clear delineation between stressed and unstressed fuels.

occurs at the same retention time as the desired feature located by the ANOVA feature selection algorithm and is drawn with a solid line in Figure 13B.

Figure 13B shows the concentration profiles of these extracted components by sample number. The first six samples are replicates of unstressed fuel, the next five were 16 hour LPR-stressed fuel, the next six 42 hour LPR-stressed fuel, and the final six 42 hour LPR-stressed fuel with added copper. It can be seen that one extracted component in this region is decreasing in concentration with LPR stress while the others remain essentially the same. This component, depicted again with a solid line, corresponds with the chromatographic feature located by ANOVA feature selection.

The loadings in the mass spectral mode for this component of the PARAFAC model are shown in Figure 14, with major peaks at m/z = 91, 115, 117, 131, 145, and 160. This extracted mass spectral data was writing the data to an appropriately formatted text file, which was then passed to the NIST Mass Spectral Search Program for the NIST/EPA/NIH Mass Spectral Library (version 2.0) which then returned automated library search results for the submitted data. A molecular structure assignment (5-ethyl-1,2,3,4-tetrahydronapthalene) was obtained via the NIST mass spectral library for the PARAFAC model component in question. This illustrates the potential diagnostic capability of this approach to detect and characterize those trace fuel constituents that have changed during use or thermal stress.

Summary of Results

When employing multidimensional chemometric techniques to perform discriminant analyses of complex fuel composition datasets, it is imperative that measures be taken to avoid unintentional weighting of results. Thus, we have to be very circumspect in how we define what constitutes a statistically significant change in composition, while avoiding interpretations that may be skewed by preconceived ideas of which chemical processes are relevant. Another aspect of this methodology that is critical is the establishment of the ability of the numerical data to accurately represent the magnitude of change, i.e., the linearity of instrumental response to compositional change.

The ANOVA analysis has been shown to be capable of extracting the significant information from complex compositional data. It was clearly shown in analysis of the oven-stressed diesel fuel samples that the chemical variations were dominated by evaporative loss of the more volatile fuel components, rather than those that are lost or gained due to fuel degradation. Utilization of LPR stress conditions minimized this effect, and allowed for a better examination of changes in fuel composition due to degradation.

Fuel degradation in samples subjected to LPR stress under the conditions described was readily observed and modeled as changes in fuel composition as monitored by GC-MS analysis of fuel samples. The ANOVA based feature selection was able to locate the features that changed from sample to sample, thus allowing for a quick evaluation of how fuel composition was altered during stress, as well as aiding in constructing hypotheses as to the mechanisms of this change.

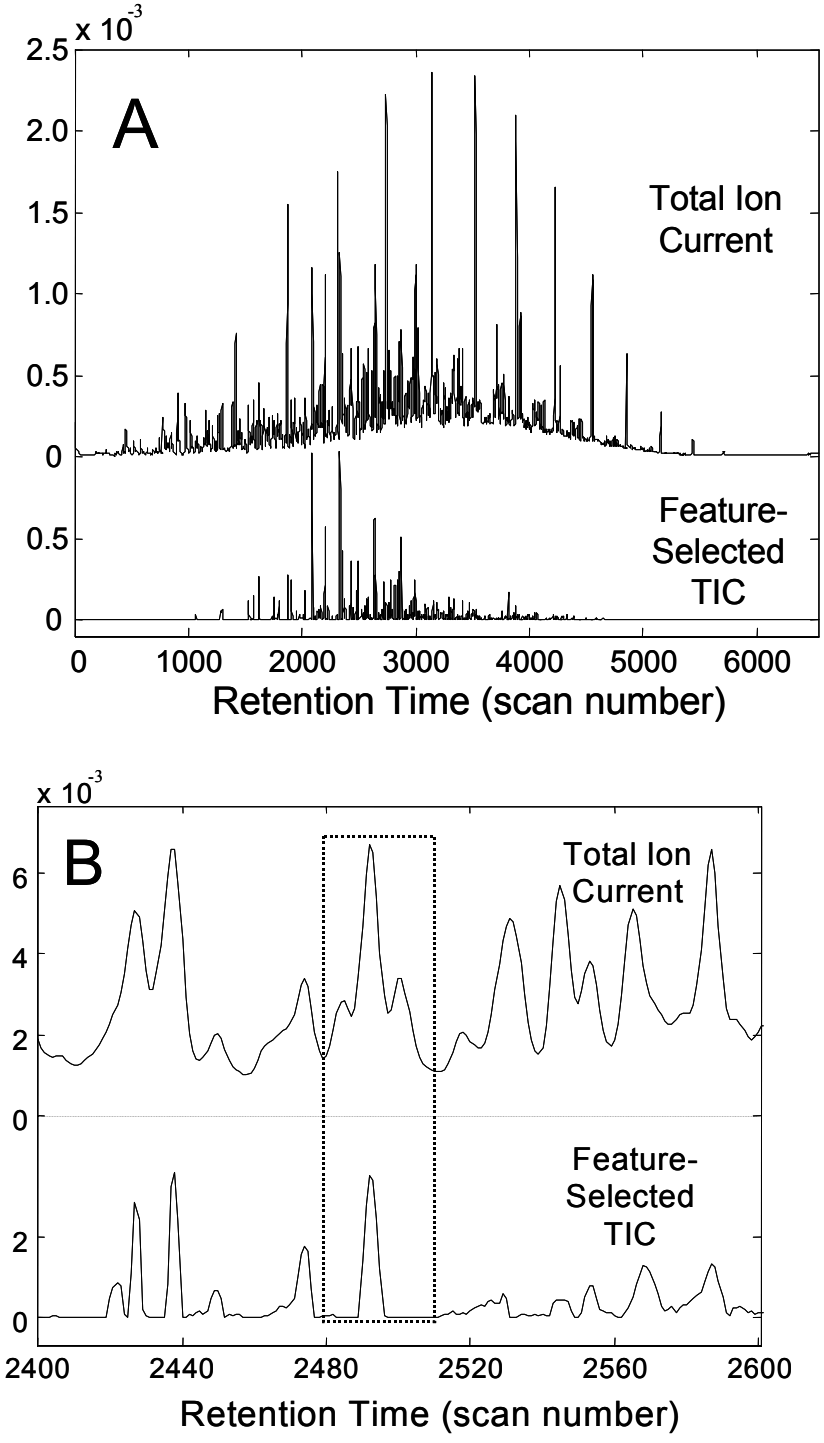

Figure 12. A) Feature-selected TIC of unstressed fuel from the LPR stress study including only data points with an ANOVA f-ratio greater than 100. Offset from the feature selected TIC is the raw (i.e. non-feature selected) TIC of the same fuel sample. B) Enlarged region of feature selected TIC.

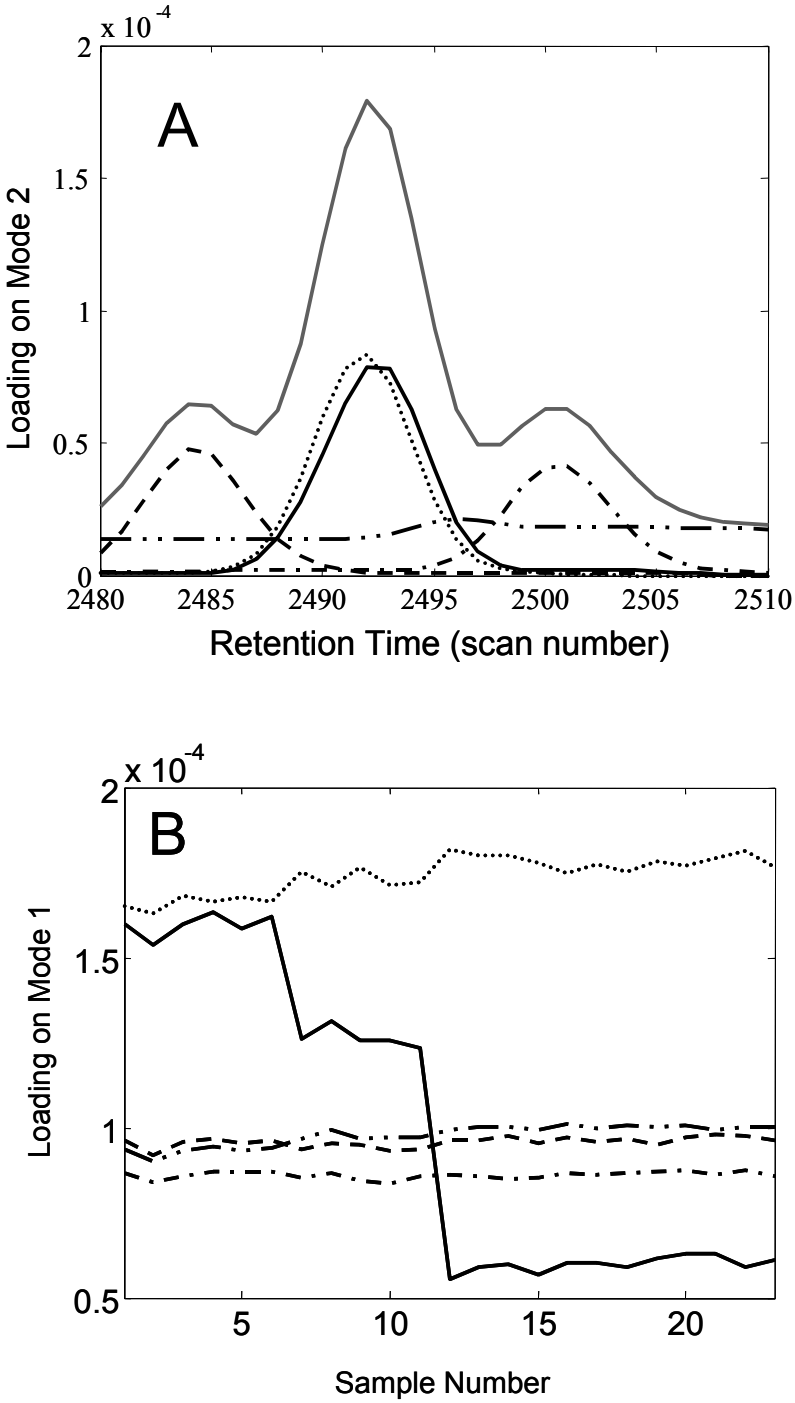

Figure 13. PARAFAC decomposition of the boxed region in Figure 12B. Unimodality and nonnegativity constraints were imposed on the chromatographic mode, and a nonnegativity constraint was imposed on the mass spectral mode. A) Resulting deconvoluted GC profiles showing four discrete Gaussian peaks. B) Deconvoluted concentration profiles, with only one component decreasing in composition with stress.

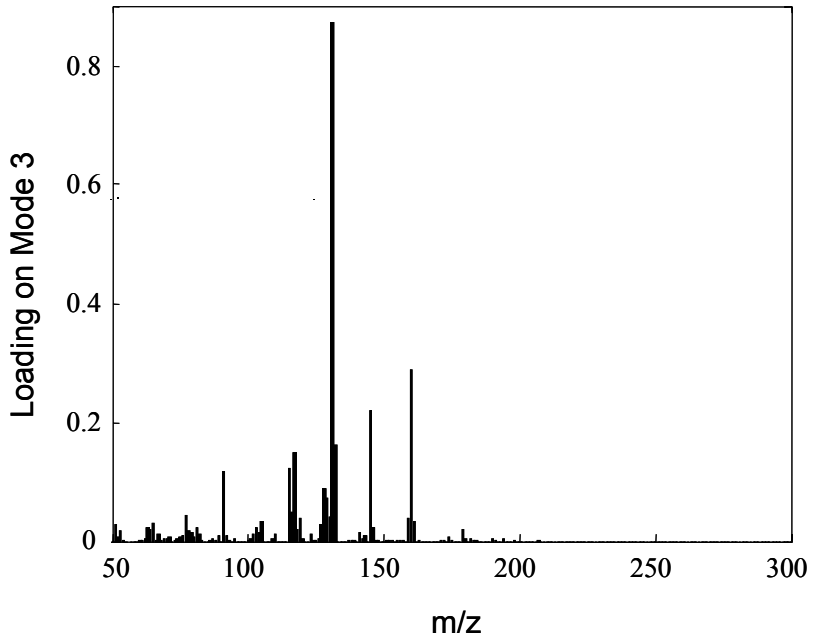

Figure 14. Mass spectral loadings of the PARAFAC model component that decreased in concentration during LPR stress. A tentative identification of this compound as 5-ethyl-1,2,3,4-tetrahydronapthalene was made via a NIST mass spectral library match.

In this experiment, it appears that this diesel fuel stressed with and without high levels of copper approached the same chemical composition "end point" although the mechanism and rate of change may have been different. This raises questions about the role of copper in fuel autoxidation, and it serves as an autoxidation accelerant without imposing significant changes in the autoxidation mechanism. Such a finding would imply that copper could be used to accelerate fuel stability testing in the laboratory.

Identification of a number of individual fuel constituents that change significantly during LPR stress may be possible through PARAFAC decomposition of local regions of GC-MS data that have been identified as significant by ANOVA-based feature selection. The potential of this approach is as a diagnostic tool, as well as a means of more completely understanding the complex processes that occur as a fuel degrades. This type of analysis could eventually provide the means to characterize compositional changes in fuels associated with degradation to an unprecedented level of detail. This level of detail and understanding of the fuel degradation process is necessary to develop reliable and robust models to predict fuel quality that are functional for more than one type of fuel. Moreover, by incorporating structure assignment functionality along with localized PARAFAC modeling and appropriate data preprocessing, it would theoretically be possible to provide a means of automating the process of analyzing the GC-MS datafiles to provide rapid compositional profiles for evaluating fuel samples.

3.3 Characterization of Fuel Blends by GC-MS and Chemometric Tools

This study was undertaken to test our hypothesis that second order chemometric tools have an even greater potential to characterize and quantify fuel components in complex mixtures. Demonstrated here is an application that illustrates the potential of three multi-way chemometric analysis tools to rapidly and effectively characterize the composition of different fuel blends.

Experimental

Fuel Blends. In the first experiment, a series of diesel fuel and light cycle oil (LCO) blends were examined. The blends were comprised of 0, 1, 5, 10, 20 and 100 percent LCO by volume, with the remainder being made up by a navy specification F-76 diesel fuel (DFM). In a second experiment, a series of samples consisting of one neat DFM sample, one DFM adulterated with home heating oil (HHO), and a blend of equal volumes of the two were examined.

GC-MS Analysis. Samples for GC-MS analysis were prepared by diluting 2 μL of each sample with 2 mL dichloromethane. An HP 6890 injector and autosampler delivered 1.0 μL aliquots of each of five replicate samples in random order to an Agilent model 5890 capillary gas chromatograph coupled to a HP 5971 mass selective detector. A split/splitless injector at 250^{o}C with a split flow ratio of 60:1 was used along with a 50 m x 0.2 mm Agilent HP-1 (dimethylpolysiloxane) capillary column. The oven temperature profile was 50^{o}C for one minute, to 290^{o}C at 10^{o}C/min, holding for seven minutes, giving a run time of 32 minutes. A solvent delay of four minutes was used which reduced the data acquisition time to 28 minutes per run. The GC-MS data that were acquired from these runs was converted from the native HP Chemstation datafiles to raw text format utilizing an in-house written MS Windows program and then imported into MATLAB for subsequent chemometric analyses.

Results and Discussion

Identification of LCO components in LCO/DFM blends. The task of detecting different fuel types in a fuel blend by gas chromatography can be limited by the overall differences in GC features from the different component fuels. As the overall differences between the compositions of the component fuels in a mixture become smaller, it becomes more difficult to discriminate the components of a blend. Thus, the greatest limitations in this approach are generally encountered in situations where a fuel may be contaminated by a small amount of a slightly different fuel. Chemometric analysis of GC data from mixtures can be successfully used to discriminate between different fuel types, but is subject to limitations imposed by the depth of information provided by the technique.

By extending this approach to a second order technique, each fuel component is more completely defined and the GC-MS can thus provide a more unique numerical representation of the fuels that comprise the sample. A significant challenge that must be overcome in the treatment of second order data, is the discrimination of statistically significant data within the complex dataset. By employing the ANOVA feature selection at each point as described above, regions of the GC-MS data can be defined that are adept at describing the chemical differences between different fuel blends. When the GC-MS of a neat DFM sample was compared to a blend of the same fuel adulterated with 20% by volume of an LCO, the ANOVA feature selection successfully extracted the total ion chromatogram (TIC) of the LCO, from the larger quantities of DFM components, as shown in Figure 15.

The individual compounds in the LCO contaminant can be also identified by computing a series of successive PARAFAC models on windowed regions of the retention time axis of the GC-MS dataset. PARAFAC models were thus constructed on successive 30 scan windows along the retention time axis, stepping the window in 20 scans increments, at each iteration. A five factor model was then calculated for each local region and LCO components were identified by locating factors in the PARAFAC model where the sample mode loadings varied significantly between the neat and adulterated DFM samples. The sample mode loadings are shown in Figure 16A, which depicts the total ion chromatograms from a series of four neat DFM samples and four DFM/LCO samples. The loading shown with the dashed line shows the most change and represents the LCO. The retention time axis loadings, in Figure 16B depicts the same three components, with the dashed line showing how the ion chromatogram of just the LCO was discriminated from the other blend components.

Comparison of this extracted ion chromatogram for the LCO with the TIC, illustrates how this approach can successfully extract the chromatographic data for a single component from a complex mixture. Accordingly, as shown in Figure 16C, the spectral loadings will yield the mass spectrum of the chemical species that produced the extracted LCO ion chromatogram peak. Submitting the spectral mode loadings of those factors to a NIST mass spectral library matching algorithm provides a list of compound matches. A partial list of components identified in this manner is shown on Figure 17, which shows a portion of the TIC and the LCO components. Ultimately, we would export these procedures to a stand-alone computer application that could start with raw GC-MS datafiles and provide the analyst a list of chemical compounds that are different between the two fuels or blends that are being compared. If a sufficient training set of fuel types were developed, it would also be possible to adopt this process to provide a means of performing automated assays of contaminated fuel samples from GC-MS data.

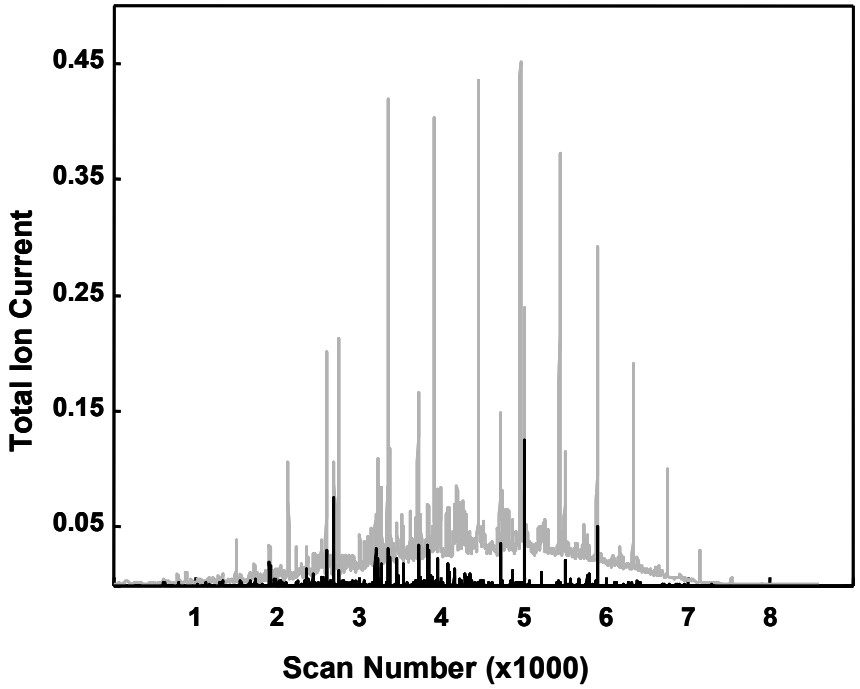

Figure 15. Total ion current chromatogram of a DFM fuel sample blended 20% by volume with LCO (gray) overlaid with feature-selected total ion current chromatogram (black).

Quantitative determinations of blending components. Since the model loadings can isolate the individual components in a fuel blend, this approach can also be used to derive quantitative information about the detected components. The overall LCO contents of the LCO / DFM blends were successfully modeled by a NPLS regression calibration. As was stated earlier, NPLS differs from standard PLS regression in that the data are not unfolded into a 2-dimensoinal matrix, but are treated as a 3-dimensional data cube and decomposed into a PARAFAC-like trilinear model. By retaining all the spatial information, much like PARAFAC, a significant improvement is obtained in the predictive power of the model. GC-MS data sets were first boxcar averaged by eight points along the retention time axis, to reduce data size and increase the speed of calculations. The predictive power of the resultant model was cross-validated by predicting the concentration of each blend with a calibration model constructed from a dataset consisting of the five GC-MS replicate analyses of each of the remaining samples. The results of these predictions are shown graphically in Figure 18, as the predicted vs actual volume percent of LCO. The overall variance of prediction represented by this graph is 14.4, although this number drops to 0.5 if the samples at either end of the LCO concentration range are excluded. This is not particularly surprising, as the calibration models used to predict both of these concentrations are extrapolated. In this manner, a quantitative determination of the amount of LCO in the DFM samples was obtained from the GC-MS analysis.

Qualitative recognition of fuels in a blend. An obvious application for GC-MS modeling of fuel mixtures would be the qualitative determination of the components that are present. A multi-way principal component analysis (MPCA) model was constructed using GC-MS chromatograms from replicate analyses of three different fuel samples, a neat DFM, a separate DFM sample known to be adulterated with an unknown quantity of home heating oil (HHO), and a mixture of equal volumes of the two. Scores from this model are shown in Figure 19, and indicate a clear delineation between the samples. An examination of the loadings on component 1 indicates the presence of HHO components from the positive loading, and those more characteristic of the DFM fuel were successfully modeled by the negative loading. The multi-way-PCA plots of the entire GC-MS datasets from these DFM and adulterated samples are depicted in Figure 20, from the loadings on the first principal component. By depicting these loadings as projections on the scan number vs m/z axes, it is evident that the GC-MS data for the DFM / HHO blends were successfully isolated, as positive loadings in Figure 20A, and the DFM itself in Figure 20B from the negative loadings of the model. This illustrates the degree to which the MPCA models can distinguish between these two very similar fuels, on the basis of their entire composition, rather than just relying on selected targeted constituents to infer the presence of the two fuel types.

Summary of Results

Significant advantages in sensitivity and selectivity can be realized when analyzing mixtures of fuels, by using multidimensional data. The ANOVA feature selection algorithm is the key to the utilization of complex datasets, such as the chromatographically resolved data obtained from a GC-MS analysis. A significant advantage of using GC-MS data over first-order spectrographic single-channel gas chromatographic measurements is the increased level of detail provided by the

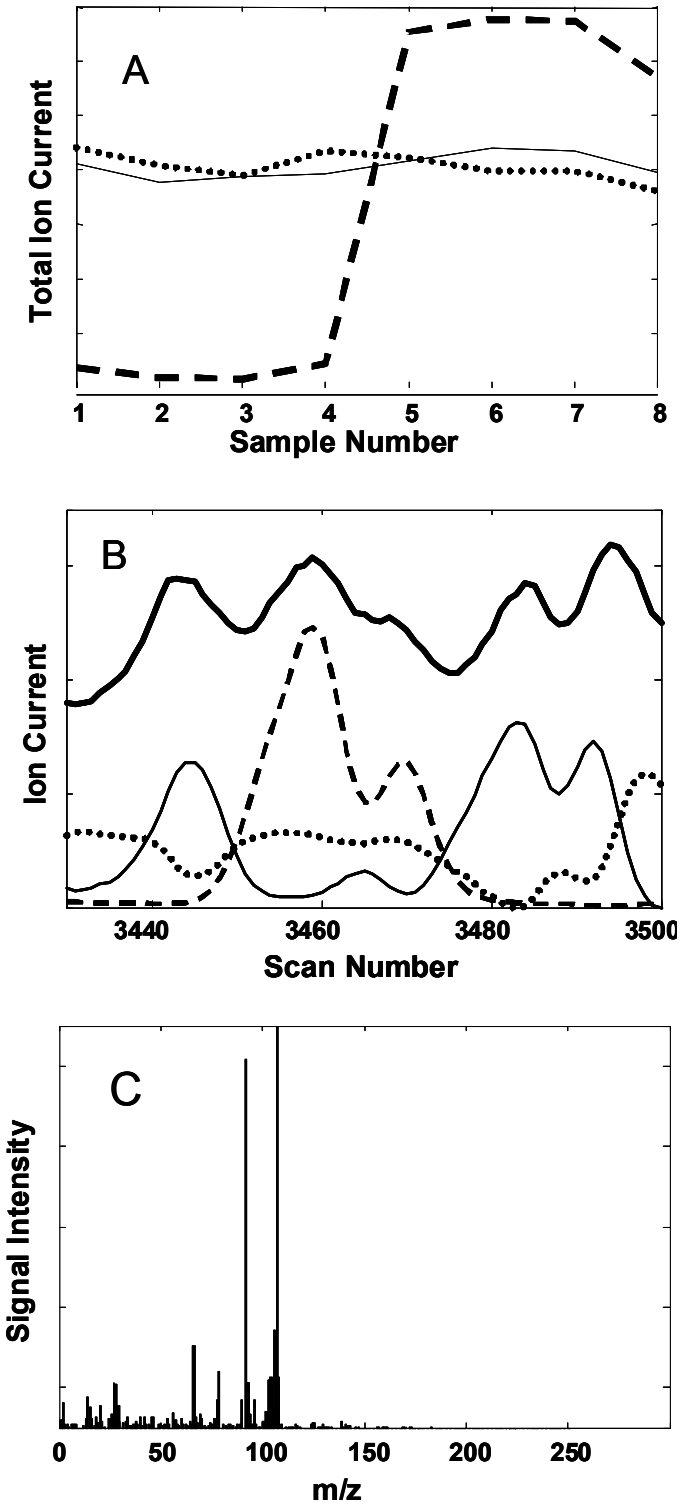

Figure 16. PARAFAC analysis of a local region of GC-MS data to deconvolve chemical components. (A) Sample mode loadings (B) Retention time axis mode loadings, with overlay of TIC in bold and (C) deconvolved mass spectrum of PARAFAC model component that changes between samples.

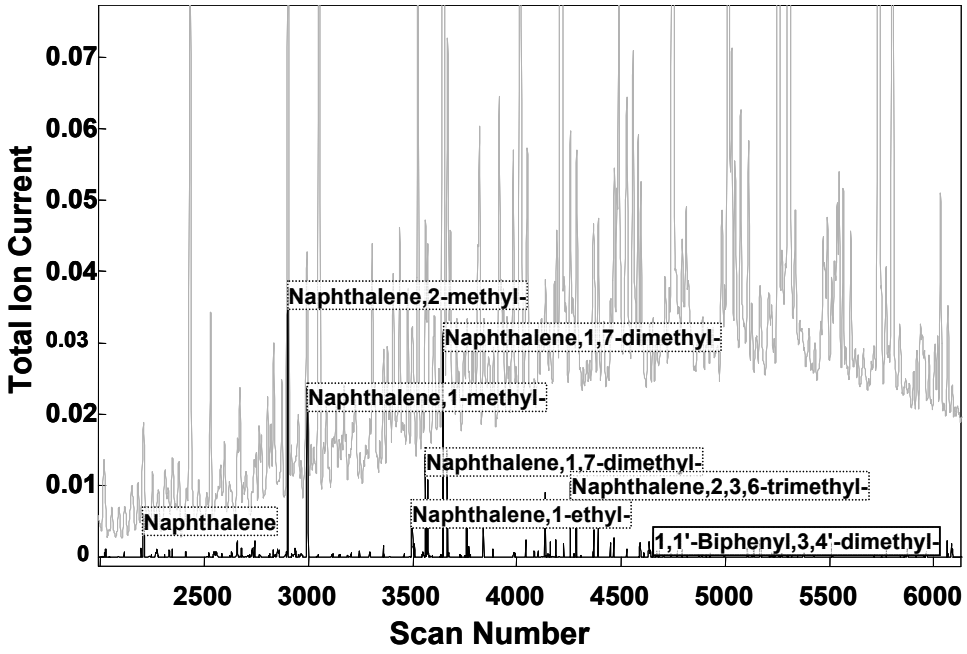

Figure 17. LCO components identified in feature-selected TIC via NIST library matching of PARAFAC-deconvolved spectra.

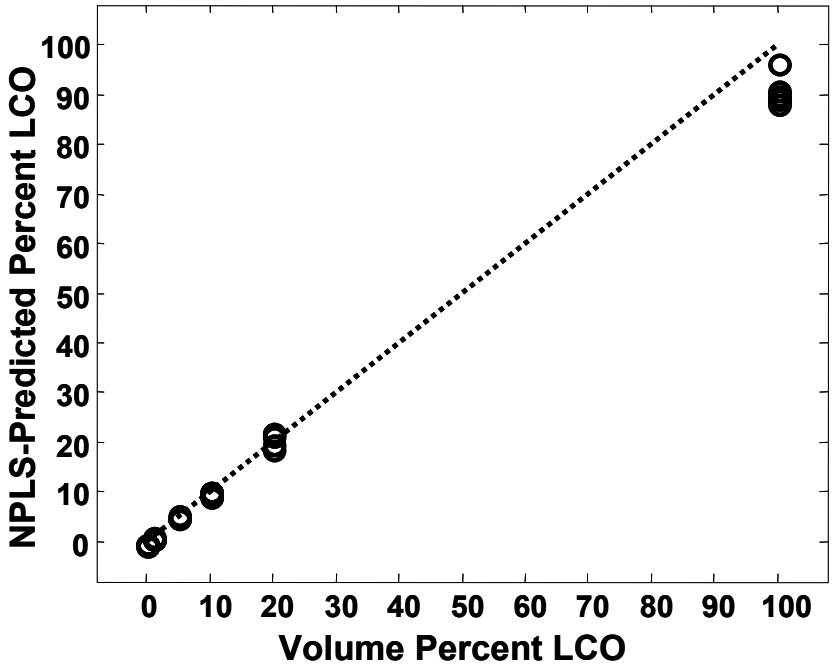

Figure 18. NPLS calibration of LCO content in DFM/LCO blends. Variance of prediction was 14.39, but reduced to 0.50 if results from prediction of concentration extremes (neat LCO and DFM samples) are omitted.

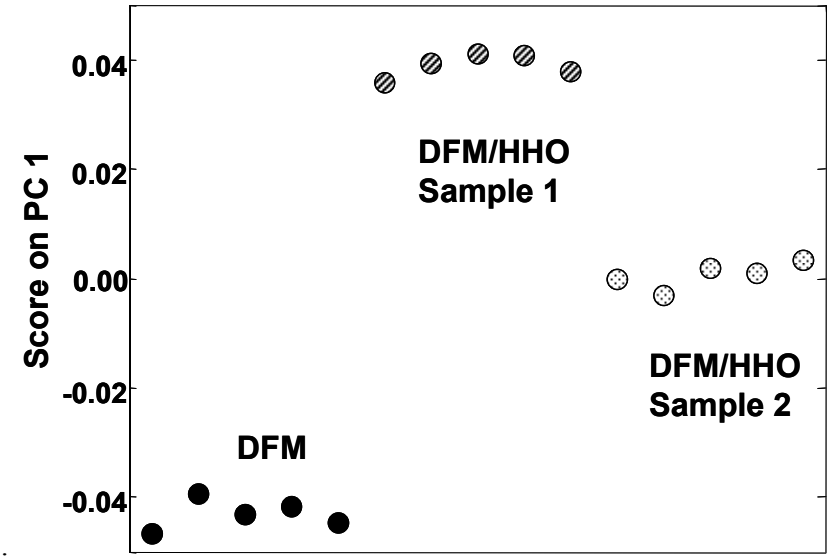

Figure 19. Scores on the first principal component from an MPCA model, showing the discrimination of three blends of Naval Distillate (DFM) with home heating oil (HHO).

analytical data. Discrimination of fuel types in mixtures is a common need in remediation of fuel spills and the examination of fuel contamination issues. Available methods for performing these types of discrimination analyses generally rely on either spectroscopic or chromatographic analyses. However, these methods are limited when the compositions of the components of a mixture overlap or are very similar. In this study, we show that many of these limitations can be overcome by including the additional dimension of compositional information provided by GC-MS. The novel multidimensional chemometric techniques described above were successfully used to analyze GC-MS data and unravel multi-component properties of fuel blends into its component parts. The sensitivity and accuracy of this approach is illustrated by successful quantitative and qualitative discrimination of the components of diesel fuel (NATO F-76) samples contaminated with light cycle oil and with another similar diesel fuel.

This approach offers the means to more effectively characterize fuel blends and contaminants, by comparison with the known fuel. If the known fuel components are not available, an estimated discrimination can still be made by comparison with typical specification fuels. This could potentially provide the capability to detect and characterize unknown fuel adulterants, by comparison with known samples of the unadulterated base fuel.

The predictive power of chemometric modeling of GC-MS data is, of course, limited to those fuel constituents that can be chromatographically separated and detected. However, the multidimensional chemometric modeling techniques described in this work would not be limited to GC-MS and could form the basis for the development of optically based sensing systems to monitor fuel cleanliness and contamination.

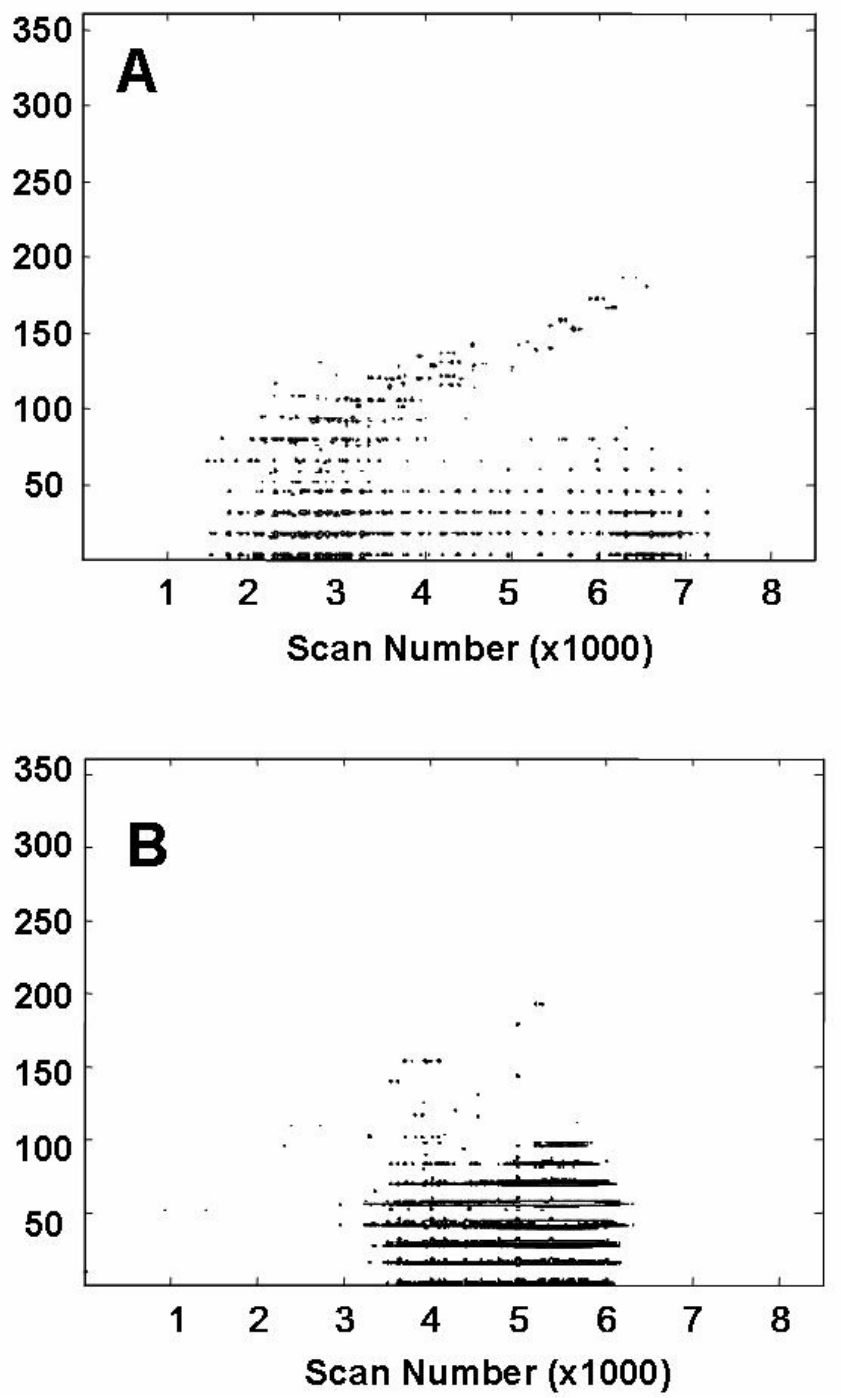

Figure 20. MPCA model of DFM/HHO blends. The two components in the mixture are clearly shown from the loadings on the first principal component. (A) positive loadings represent the home heating oil and , (B) negative loadings which represent the diesel fuel.

4.0 EVALUATING THE PREDICATIVE POWERS OF SPECTROSCOPY AND CHROMATOGRAPHY FOR FUEL QUALITY ASSESSMENT

Currently, fuel quality in the field or onboard ship is assessed with a series of traditional ASTM fuel test procedures. A sensor-based device to perform these tests would not only provide significant savings in cost and manpower, but reduce the hazards associated with handling large volumes of fuel samples. It would also provide faster, and in many cases, more consistent results. This phase of the program was thus focused on developing sensing technologies to perform fuel quality assessment and diagnostics. This technology is based upon the prediction of critical fuel properties from an array of optical and other specialized sensors. These predictions will take advantage of predictive models derived from chemometric analysis of the data stream.

The predictive power of chemometric regression models based on chromatographic data are compared with those generated from NIR and Raman spectroscopic data to evaluate the potential of these analytical techniques for the development of an advanced fuel quality sensor system. A training set of fuel samples from around the world was acquired, with complete compositional and specification test results. These samples were analyzed by NIR, Raman and GC-MS. These data were evaluated for their ability to predict various fuel properties via PLS as part of an effort directed towards developing robust, sensor-based fuel quality assessment methodologies.

Experimental

Fuel sample set. A set of 45 jet fuels that were sampled from around the world, were used in this initial survey. The set consisted of Jet A (11 samples), Jet A-1 (22 samples), JP-8 (9 samples), JP-5 (2 samples) and a petroleum (Stoddard) solvent (1 sample). The samples were supplied with measured values for 28 fuel specification properties, and all fuel samples met the appropriate specifications. The range of property values reported for this fuel set are given in Table 5.

NIR Spectroscopy. Near-infrared spectra were obtained with a Cary model 5E spectrophotometer. Supracell cells with path lengths of 10 and 1 mm were used. Initial spectra were obtained from 300 to 2300 nm, with a resolution of 1 nm. For chemometric analysis, the spectral region from 1000 to 2300 nm was used. Repeatability of spectra was excellent, with the exception of some baseline variations observed when the 1 mm sample cell was used, presumably due to slight differences in positioning the cell in the beam. These baseline variations with the 1 mm cell data were corrected using the multiplicative scatter correction function in the PLS Toolbox for MATLAB prior to multivariate analysis. Preliminary comparisons between the 1 mm and 10 mm data indicated no significant advantage to the 1 mm cell, and so its use was discontinued. Data were collected with the Cary software provided with the instrument, and exported in comma separated value (CSV) format. The resultant numerical representations of the spectra were combined in one array.

Raman Spectroscopy. Raman spectra for a 30 fuel subset of the total sample set were provided by Real-Time Analyzers, Inc. (Middletown, CT), and were acquired with a portable scanning FT-Raman spectrometer of their manufacture. Spectra were acquired from 500 to 3500 cm^{-1} with a resolution of 1 cm^{-1}.

GC-MS Analysis. Samples for GC-MS analysis were prepared by diluting 2 µL of each sample with 2 mL dichloromethane. An autosampler injected 1.0 µL aliquots of each of five

replicate samples in random order to an Agilent model 5890 capillary gas chromatograph coupled to a HP 5971 mass selective detector. A split/splitless injector at 250°C with a split flow ratio of 60:1 was used along with a 50 m x 0.2 mm Agilent HP-1 (dimethylpolysiloxane) capillary column. The oven temperature profile was 50°C for one minute, to 290°C at 10°C/min, holding for seven minutes, giving a run time of 32 minutes. A solvent delay of four minutes was used which reduced the data acquisition time to 28 minutes per run. Masses were scanned from m/z of 40 to 240. The GC-MS data that were acquired from these runs was converted from the native HP Chemstation data files to raw text format utilizing an in-house written MS Windows program. The chromatograms were then aligned to one another to minimize retention time variations from sample to sample via a standalone MS Windows program implementing the correlation optimized warping algorithm described by Vest Nielsen. (available for download at *http://www.biocentrum.dtu.dk/mycology/analysis/cow/*)

Chemometric Regression. PLS and principal components regression (PCR) was performed utilizing the NIR spectra, Raman spectra, GC total ion current chromatograms, and unfolded GC-MS chromatograms against the 28 measured fuel properties. Both PLS and PCR are inverse least squares regression models that use factor analysis to reduce the spectral or chromatographic data prior to regression.[33] PCR projects the input data onto a lower dimensional subspace calculated to most efficiently represent the sample-to- sample variation contained within the calibration data, whereas PLS projects the input data onto a lower dimensional subspace calculated to best represent the covariance between the calibration data and corresponding reference values. These two regression techniques were chosen for consideration as they are well established, well characterized, and widely implemented in various software packages. Additionally, multiway partial least squares regression was used to regress GC-MS datasets against the provided fuel properties for each of the 45 fuels in the sample set.

NIR and Raman spectra were assembled into matrices in which each row was a spectrum of a different fuel sample. The acquired dataset for GC-MS analysis consisted of a series of two-dimensional GC-MS chromatograms, one for each sample analyzed, stacked on each other to form a three-dimensional array, or cube of data. Total ion current (TIC) chromatograms were constructed by summing each GC-MS dataset along the m/z axis. "Unfolded" GC-MS chromatograms were created by reshaping the data matrix for each GC-MS chromatogram into a single row vector. Prior to unfolding, each GC-MS chromatogram was boxcar averaged with a window of five points.

PLS and PCR algorithms were implemented utilizing the PLS Toolbox. Calibration models were evaluated utilizing "leave-one-out" cross validation in which the property value of each sample is predicted utilizing a calibration model built from all of the other data. Regression models were built utilizing from one to ten latent variables (or components) and the model with the lowest root mean square error of cross validation (RMSECV) was chosen for inclusion into the results. A limit of 10 latent variables was imposed to guard against over-fitting the data with excessively complex models, and provided us with a maximum ratio of roughly five fuel samples per latent variable a regression model. For purposes of comparison between models of different properties, RMSECV values were normalized by the mean observed for the fuel property they were predicting.

[33] Richard Kramer, "Chemometric Techniques for Quantitative Analysis," Marcel Dekker, New York, 1998.

ASTM	Property Name	min	max	range	mean	std
D4052	density at 60 ºF, g/ml	0.78	0.82	0.04	0.80	0.01
D93	flash point (P-M), ºF	105.00	154.00	49.00	119.69	11.94
D3828	flash point (mini), ºF	103.00	144.00	41.00	120.11	10.35
D5972	freeze point, ºC	-72.00	-44.00	28.00	-52.31	5.62
D5949	pour point, ºC	-80.00	-60.00	20.00	-69.20	2.84
D2622	total sulfur, ppm	7.00	2453	24460	417.64	432.21
D1840	naphthalenes, vol %	0.00	3.80	3.80	1.30	0.76
D1319	aromatics, vol %	11.80	22.00	10.20	17.88	2.13
D6379	aromatics, vol %	13.00	24.40	11.40	19.57	2.40
D1319	saturates, vol %	75.80	87.00	11.20	80.50	2.13
D1159	olefins, vol %	0.06	1.53	1.47	0.35	0.25
D1319	olefins, vol %	0.70	2.30	1.60	1.62	0.35
D3701	hydrogen, weight %	13.71	14.47	0.76	14.15	0.19
D4809	net heat content, btu/lb	18331	18589	258	18506	52.08
D445	viscosity 20 ºC, mm^2/sec	1.30	3.00	1.70	1.78	0.30
D445	viscosity -20 ºC, mm^2/sec	2.70	6.20	3.50	4.18	0.81
D445	viscosity -40 ºC, mm^2/sec	4.80	14.60	9.80	8.59	2.38
D1218	refractive index	1.44	1.46	0.02	1.45	0.00
D2624	conductivity, pS/m	0.00	395.00	395.00	93.11	101.11
D3242	acid number, mg KOH/g	0.0000	0.0200	0.0200	0.0055	0.0035
D3241	thermal stability, ºF	265.00	370.00	105.00	286.89	16.90
D5001	lubricity, mg/L	0.54	0.71	0.17	0.62	0.04
D86	initial boiling point, ºF	294.10	362.80	68.70	318.17	15.83
D86	10% distillation, ºF	329.10	388.60	59.50	347.66	15.79
D86	20% distillation, ºF	335.20	400.00	64.80	358.81	16.52
D86	50% distillation, ºF	346.40	439.00	92.60	391.34	20.45
D86	90% distillation, ºF	372.40	488.30	115.90	454.68	22.65
D86	final boiling point, ºF	386.80	521.70	134.90	481.01	25.00

Table 5. Summary of fuel property data ranges and standard deviations for each tested property.

Six preprocessing strategies were examined for each dataset. For spectroscopic data, these strategies were as follows: 1) no preprocessing, 2) second derivative, 3) autoscaling, 4) mean-centering, 5) second derivative followed by autoscaling, and 6) second derivative followed by mean-centering. Second derivative transformation was implemented through the Savitsky-Golay filter algorithm in the PLS Toolbox. For chromatographic data, the preprocessing strategies tested were as follows: 1) no preprocessing, 2) normalization, 3) autoscaling, 4) mean-centering, 5) normalization followed by autoscaling, and 6) normalization followed by mean-centering. Normalization was implemented by dividing each individual chromatogram by its Euclidean norm, and was implemented to minimize any injection volume variation from run to run. Thus, for each preprocessing scheme, and each regression technique, an optimized regression model using up to 10 latent variables was calculated and the RMSECV of that model was recorded.

Additionally, N-PLS was used to build regression models to predict fuel properties with entire GC-MS chromatograms. GC-MS data was boxcar averaged along the retention time axis with a window of ten points and the mass spectral axis of the data was truncated to the first 100 masses acquired (m/z of 40 to 139) in order to speed calculations.

Results and Discussion

The fuel sample densities predicted from PLS regression of the Raman spectra are plotted against the measured values in Figure 21. Reasonably good agreement was obtained as shown when the data were mean centered and regressed with ten latent variables. The predicted vs aromatic contents of the fuel samples from PLS regression of NIR spectra are shown in Figures 22 and 23, for measurements obtained by the HPLC method[34], ASTM D6379, and the fluorescent indicator absorption (FIA) method[35], ASTM D1319, respectively. The PLS regressions were performed on the mean centered data, using seven latent variables. As shown, good agreement was obtained between the predicted and measured values for aromatic content by HPLC and by the FIA method. However, when the HPLC measurements are plotted against the corresponding FIA measurements in Figure 24, it is evident that the HPLC values were systematically higher. This illustrates the ability of PLS correlation modeling to derive reasonably accurate predictions from the same set of spectral data for two different measurements of a single property, even if the results of those two techniques are not in complete agreement with each other. Clearly, both the HPLC and the FIA methods are self-consistent, but it is important to specify which ASTM method is being used, since the models derived in this manner are only representative of the data used in the training set.

Assessment of prediction errors. The error of prediction of a chemometric regression model is a function of the uncertainty in the original ASTM reference values as well as of the error associated with the analytical technique used to acquire spectroscopic or chromatographic data utilized for model building. One would expect that the error in prediction of a good regression model would be comparable in magnitude to the uncertainty of the reference values used to construct it. Accordingly, the chemometric regression models were first evaluated to see how their rates of error compared to the reproducibility and repeatability values of the respective ASTM methods that were used to acquire the reference measurements. Reproducibility and repeatability values were calculated using the formulas published in the method specifications and the mean property values observed across the entire set of fuel samples. These values are compiled in Table 6, along with the root mean errors of cross validation for the chemometric regression models constructed. The property normalized RMSECV values that were 10% or less of the measured values for the PLS and PCR models are plotted, along with the published ASTM repeatability values normalized by the mean measured values for each property in Figure 25. An examination of Table 6 shows that the PLS model RMSECV values do, in fact, tend to be roughly similar in magnitude to the ASTM method values, with a few notable exceptions. The corresponding PCR model RMSECV values were similar. Predictions made for sulfur content and conductivity exhibited much greater error than would be expected from the ASTM method uncertainty alone. This is unsurprising, as none of the analytical techniques examined directly probe these fuel properties. Also notable is the fact that both of the flash point measurement models exhibit significantly smaller error than the ASTM method uncertainty would imply. The reasons for this are unclear, but could be the result of overfitting in the regression model, higher

[34] ASTM. Standard Test Method for Determination of Aromatic Hydrocarbon Types in Aviation Fuels and Petroleum Distillates – High Performance Liquid Chromatography Method with Refractive Index Detection. *In Annual Book of ASTM Standards*; ASTM: Philadelphia, PA, 2002; Vol. 05.04, ASTM D6379-04.

[35] ASTM, Standard Test Method for Hydrocarbon Types in Liquid Petroleum Products by Fluorescent Indicator Adsorption. *In Annual Book of ASTM Standards*; ASTM: Philadelphia, PA, 2002; Vol. 05.04, ASTM D1319-03.

than normal precision from the analytical lab that performed the measurements, or some combination of factors.

Properties amenable to predictive modeling. Table 7 contains RMSECV values for PLS and PCR model predictions and predictions, normalized to mean property value for the sake of comparison across different properties. The worst performing models are those for olefins (ASTM D1319) naphthalenes, acid number, total sulfur, olefins (ASTM D1159/D27), and conductivity, all giving RMSECV values that were greater than 20% of the mean property values being predicted (Table 5). A number of models, however, gave RMSECV values that were less than ten percent of the mean property value, indicating potential for inclusion into the proposed automated fuel assessment methodology. Among these properties were those of interest in fuel quality assessment, shown in Table 1: density, freeze point, pour point, flash point, aromatic content, and viscosity.

PLS vs PCR modeling efficiencies. From Table 7, one can see that there seems to be little difference between the results obtained from each regression method. The ratios of PLS/PCR RMSECV values, shown in Table 8 clearly illustrate that PLS and PCR models perform with comparable accuracy, although when PLS models are better, they tend to be better by a slightly larger margin than that of PCR models that are better their corresponding PLS model. As the number of latent variables required to adequately model a particular property increases, so does the complexity of the resultant model and its specificity for the particular fuels that constitute the training set. As a consequence, models with high numbers of latent variables tend to fail when applied to fuels that are not similar to those used to develop that particular model. Models developed with high numbers of latent variables are generally referred to as over-fitting the data. It is therefore desirable to construct models that adequately relate to the property of interest with as few latent variables as possible, trading off precision for robustness. Table 9 lists the optimum number of latent variables required for each property model shown. An examination of this Table shows that in general, the model that performed best for each property, also required the most latent variables, and thus the greatest model complexity, regardless of regression method. It is apparent, however, that PCR models requiring high numbers of latent variables return slightly less improvement in terms of RMSECV versus cases where PLS models require high numbers of latent variables. For example, the PCR model for flash point (D93) requires six extra latent variables to obtain an RMSECV that is 4% lower than the 3 latent variable PLS model. Conversely, the PLS model for pour point requires only 3 extra latent variables to obtain an RMSECV that is 7% lower than the seven latent variable PCR model.

Comparison of analytical techniques. Next to be considered is the question of which analytical technique provides the best data for chemometric prediction of fuel properties. Table 10 lists the optimum RMSECV for each of the three analytical techniques examined. RMSECV values obtained from calibrations using GC or spectroscopic data were essentially comparable, except in the prediction of saturate content, aromatic content, and freeze point, where NIR performed substantially better. In fact, from Table 10 it can be seen that calibrations constructed with NIR or Raman data generally performed slightly better than, or comparably to those constructed with GC data, with exceptions for freezing point, distillation temperatures, and viscosity where calibrations using GC data performed slightly better.

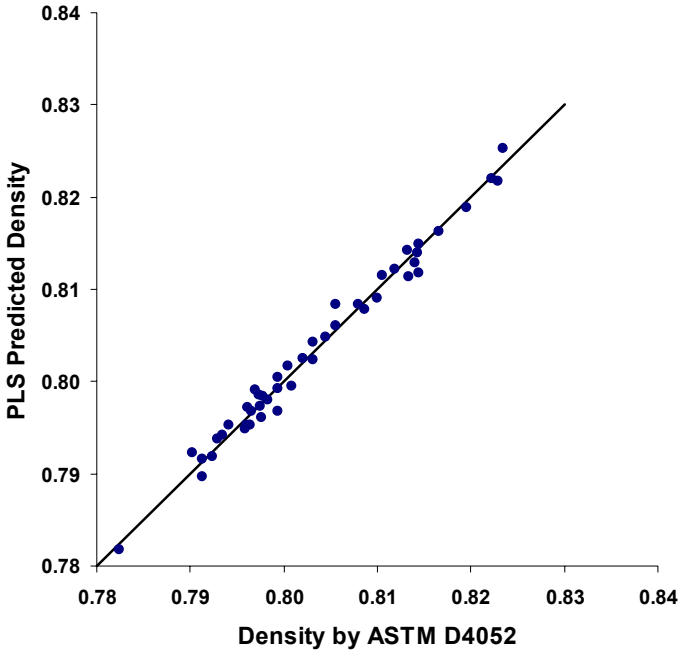

Figure 21. Density of the jet fuel sample set predicted by PLS regression of Raman spectra using ten latent variables, versus density measured by ASTM D4052

.

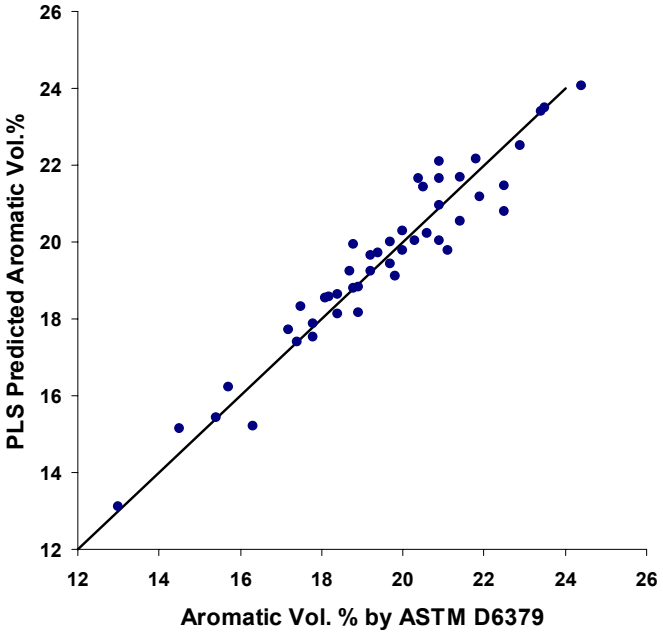

Figure 22. Jet fuel sample aromatic content predicted by PLS regression of NIR spectra using seven latent variables, versus aromatic content measured by ASTM D6379 (HPLC method).

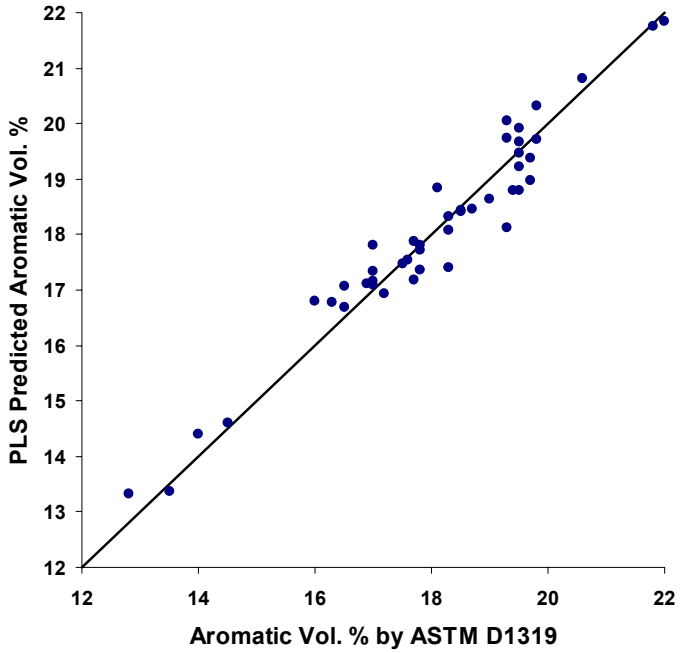

Figure 23. Jet fuel sample aromatic content predicted by PLS regression of NIR spectra using seven latent variables, versus aromatic content measured by ASTM D1319 (FIA method).

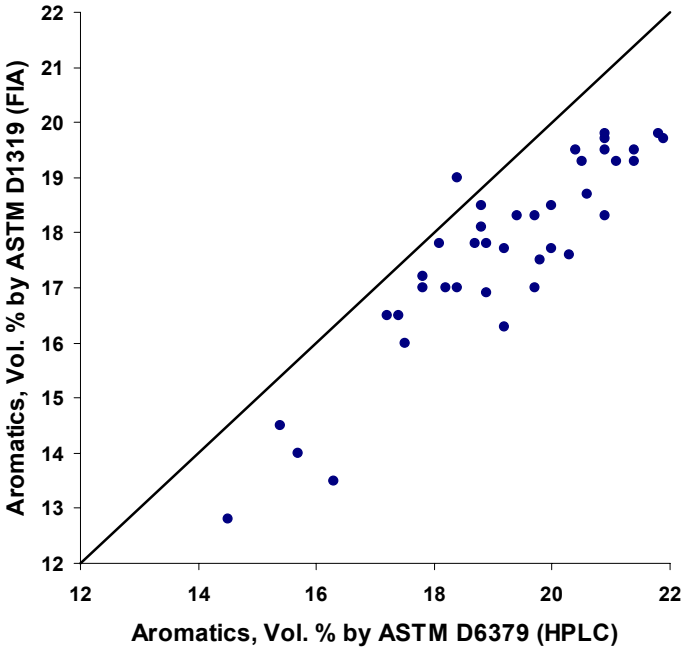

Figure 24. Aromatic content in the jet fuel sample set, measured by ASTM D6379 vs. ASTM D1319.

Regressing fuel properties against unfolded GC-MS data led to some slight improvements in prediction of freeze point and pour point, but otherwise performed somewhere in between regression models utilizing total ion current chromatograms and those using NIR spectra. N-PLS regression models utilizing averaged GC-MS data sets performed in a comparable fashion or worse than other regression models. In this study, no advantage was seen in utilizing N-PLS regression over standard PLS on unfolded data, especially in models with the lowest RMSECV values, such as density and refractive index, where N-PLS gave RMSECV values 5 and 16 times greater than those constructed with unfolded GC-MS data.

Data preprocessing methods. The effects of the preprocessing algorithms considered in this study were inconsistent from property to property, decreasing the RMSECV in many cases but raising it in others. For example, mean centering lowered RMSECV values in PLS calibrations for flash point, lubricity, and viscosity at -40 ºC while slightly raising RMSECV in PLS calibrations for saturate and aromatic content. It is likely that this variability may be reduced when a larger training set of fuels is considered. In general, however, results from mean centering provided either the best RMSECV, or an RMSECV that was not more than 10% greater than the processing scheme that did. In all cases, applying a second derivative transformation to the spectroscopic data resulted in a significant increase in RMSECV. Autoscaling provided results that were comparable or slightly worse than mean centering in all but a few cases.

Summary of Results

Feasibility of chemometric prediction of a number of critical fuel properties from measured capillary gas chromatograms, NIR spectra, and Raman spectra has been demonstrated. Root mean errors of cross validation of predicative models for critical properties of interest were less than 10% of observed mean property values, and commensurate with uncertainties expected from the ASTM methods utilized to acquire reference values for this study. The findings of this study do not indicate that there were any statistically significant differences between NIR and Raman spectroscopy in terms of regression model performance. Thus, a system based solely on either NIR or Raman spectral data should perform equally well, although a system based on both GC and spectral instruments could provide some improvement, particularly in the prediction of freeze point and viscosity.

Predictions based on unfolded GC-MS chromatograms and N-PLS regression of whole GC-MS chromatograms failed to yield significant improvement over predictions based on calibration models utilizing total ion current chromatograms, or capillary gas chromatography. A sensor-based fuel quality assessment system could in theory be augmented with specialized sensors to allow evaluation of properties that are not amenable to chemometric prediction from chromatography or spectroscopy alone, such as conductivity, total sulfur, and acid number.

ASTM	Property	ASTM Method Errors		PLS Minimum RMSECV		
		Reprod.	Repeat.	NIR	Raman	GC
D4052	Density	0.0005	0.0001	0.0026	0.0018	0.0031
D93	Flash Pt. (PM)	32.0	33.3	8.8	8.9	7.1
D3828	Flash Pt. (mini)	37.0	33.3	7.8	7.5	7.4
D5972	Freeze Pt.	1.3	0.7	3.6	4.2	3.0
D5949	Pour Pt.	6.8	3.4	2.7	2.2	2.1
D2622	Sulfur	30	21	283	233	419
D1840	Naphthalenes	0.069	0.051	0.47	0.41	0.55
D1319	Arom., FIA	2.70	1.30	0.66	0.92	1.32
D6379	Arom., HPLC	1.897	0.938	0.64	1.09	1.48
D1319	Saturates	4.40	1.40	0.75	1.20	1.37
D1159	Olefins	0.40	0.20	0.21	0.34	0.22
D1319	Olefins, FIA	2.10	0.60	0.34	0.48	0.31
D3701	Hydrogen	0.11	0.09	0.11	0.20	0.12
D4809	Heat Content	77.4	22.9	27.0	48.0	40.4
D445	Visc. 20ºC	-	-	0.25	0.30	0.24
D445	Visc.-20ºC	-	-	0.47	0.47	0.39
D445	Visc.-40ºC	-	-	1.16	1.00	0.86
D1218	Ref. Index	0.0005	0.0002	0.0012	0.0019	0.0013
D2624	Conductivity	17	5	77	92	87
D3242	TAN	0.0030	0.0010	0.0034	0.0030	0.0034
D3241	Thermal Stab.	-	-	46	58	47
D5001	Lubricity	0.070	0.046	0.037	0.038	0.033
D86	IBP	15.3	6.3	11.0	11.4	9.6
D86	10%	10.8	5.1	9.2	7.8	5.7
D86	20%	13.9	5.3	8.5	6.9	5.1
D86	50%	24.2	9.0	8.9	15.2	10.5
D86	90%	11.6	5.4	14.0	13.3	10.9

Table 6. Comparison of Regression model root mean error of cross-validation (RMSECV) calculated from mean observed value for each property over all samples, with the published ASTM method reproducibility and repeatability.

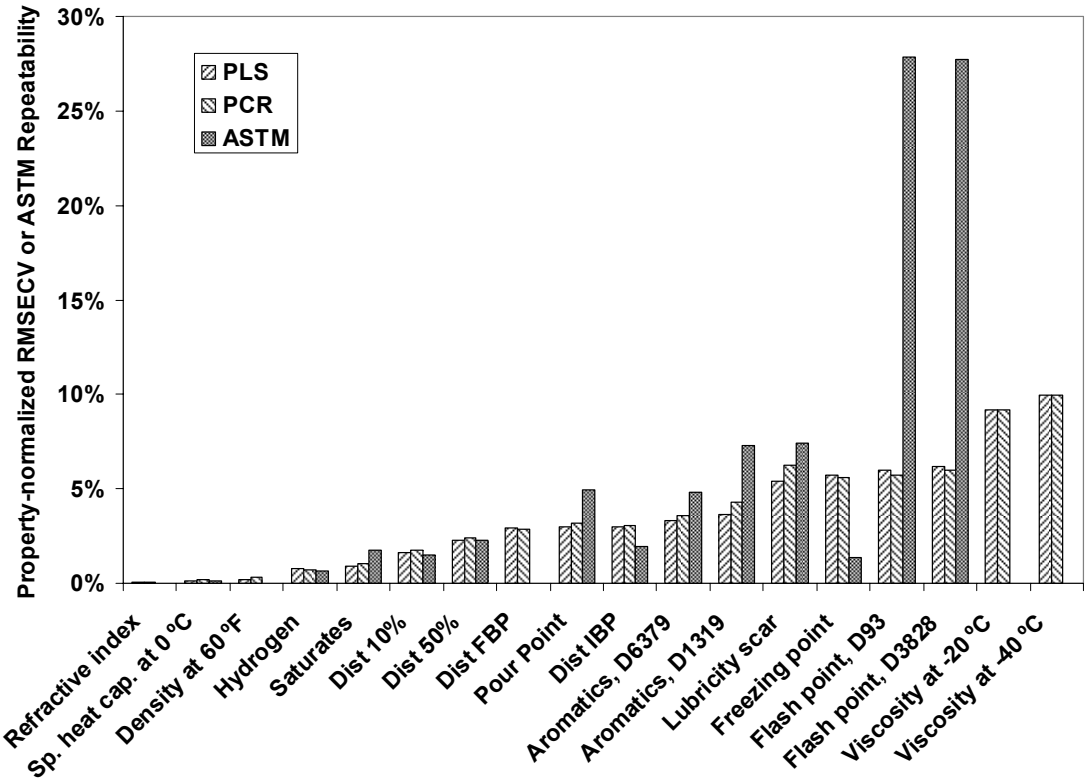

Figure 25. RMSECV values for PLS and PCR models, compared to the corresponding ASTM method repeatability for each property, normalized by the mean property values measured for this fuel dataset.

5.0 CONCLUSIONS

5.1 Chemometric Analysis of Chromatographic Data

The findings of this study have shown that chemometric analysis can be successfully employed to establish a relationship between the composition of a particular fuel to its suitability for use. With proper preprocessing, the tendency of jet fuels from one particular refinery to cause catastrophic engine failures through excessive coking, were successfully classified on the basis of data obtained through gas chromatography with flame ionization detection. Although this approach proved successful in the scenario examined, it is likely that the accuracy of a classification model developed for one set of fuels will suffer when applied to a new set of fuels obtained some time later. This is due to normal variations in fuel feed stocks and refinery operating parameters that are difficult to model explicitly. Thus, in addition to proper instrument maintenance and data pretreatment, classification model maintenance and calibration against updated fuel sample sets are required to maintain high accuracy of such a classifier.

Property	RMSECV PLS	RMSECV PCR
Refractive index	0.00085	0.000941
Sp. heat cap. at 0 ºC	0.00146	0.00172
Density at 60 ºF	0.00219	0.00327
Hydrogen	0.00765	0.00735
Saturates	0.00929	0.0103
Dist 10%	0.0164	0.0174
Dist 50%	0.0226	0.0244
Dist FBP	0.0291	0.0289
Pour Point	0.0297	0.0321
Dist IBP	0.0302	0.0304
Aromatics, D6379	0.0329	0.0357
Aromatics, D1319	0.0366	0.0429
Lubricity scar	0.0540	0.0624
Freezing point	0.0570	0.0559
Flash point, D93	0.0597	0.0575
Flash point, D3828	0.0615	0.0601
Viscosity at -20 ºC	0.0920	0.0916
Viscosity at -40 ºC	0.0995	0.0996
Viscosity at 20 ºC	0.136	0.134
Thermal stability	0.165	0.163
Olefins, D1319	0.194	0.192
Naphthalenes	0.319	0.329
Total sulfur	0.537	0.653
Acid number	0.545	0.545
Olefins, D1159/D27	0.605	0.576
Conductivity	0.840	0.909

Table 7. Summary of PLS and PCR calibration results. The lowest observed RMSECV for each property (normalized to mean property value) is displayed and these results are sorted from lowest to highest of the PCR results.

A potential route to address this issue is through the use of higher-order analytical instrumentation and multi-way chemometric algorithms.[27-32] These techniques, in principal, allow for the deconvolution of independently varying components from sample to sample, regardless of the presence of unknown interfering chemical species, thus vastly increasing the selectivity and power of the entire analytical method. It has been shown that expanding fuel analysis to a three dimensional analytical technique such as gas chromatography with mass spectrometry detection, reduced model dependence on fuel source by allowing the elucidation of trace level changes in fuel composition down to the individual compound level. This type of analyses could provide a means to characterize compositional changes in fuels associated with degradation to an unprecedented level of detail.

Property	Ratio	Property	Ratio
Density at 60 ºF	0.67	Viscosity at 20 ºC	1.01
Flash point D93	1.04	Viscosity at -20 ºC	1.00
Flash point D3828	1.02	Viscosity at -40 ºC	1.00
Freezing point	1.02	Refractive index	0.91
Pour point	0.93	Conductivity	0.92
Total sulfur	0.82	Acid number	1.00
Naphthalenes	0.97	Thermal stability	1.01
Aromatics, D1319	0.85	Lubricity scar	0.87
Aromatics, D6379	0.92	Dist IBP	0.99
Saturates	0.90	Dist 10%	0.94
Olefins, D1159/D27	1.05	Dist 20%	0.97
Olefins, D1319	1.01	Dist 50%	0.93
Hydrogen content	1.04	Dist 90%	1.05
Sp. heat cap. at 0 ºC	0.85	DIST FBP	1.01

Table 8. Comparison of PLS versus PCR model performance. Listed are the ratios of lowest PLS model RMSECV to lowest PCR model RMSECV for each fuel property

roperty	PLS	PCR	Property	PLS	PCR
Density at 60 ºF	10	10	Viscosity at 20 ºC	2	6
Flash point D93	3	9	Viscosity at -20 ºC	1	1
Flash point D3828	4	9	Viscosity at -40 ºC	3	7
Freezing point	5	10	Refractive index	7	8
Pour point	10	7	Conductivity	3	4
Total sulfur	10	2	Acid number	1	1
Naphthalenes	8	5	Thermal stability	1	1
Aromatics, D1319	8	8	Lubricity scar	8	5
Aromatics, D6379	10	9	Dist IBP	3	7
Saturates	8	8	Dist 10%	4	9
Olefins, D1159/D27	6	7	Dist 20%	4	9
Olefins, D1319	1	3	Dist 50%	5	9
Hydrogen	7	8	Dist 90%	3	9
Sp. heat cap. at 0 ºC	6	4	DIST FBP	10	9

Table 9. Number of latent variables utilized in best PLS and PCR models.

Property	ASTM Spec.	GC	NIR	Raman
Refractive index	D1218	**0.0009**	**0.0009**	0.0013
Density at 60 ºF	D4052	0.0038	0.0032	**0.0022**
Flash point	D93	0.0597	**0.0734**	0.0747
Flash point	D3828	**0.0615**	0.0652	0.0627
Freeze point	D5972	**0.0570**	0.0699	0.0810
Pour point	D5949	**0.0298**	0.0394	0.0322
Naphthalenes	D1840	0.4321	0.3700	**0.3191**
Aromatics	D1319	0.0739	**0.0367**	0.0513
Aromatics	D6379	0.0759	**0.0329**	0.0559
Saturates	D1319	0.0170	**0.0093**	0.0149
Olefins	D1159/D27	0.6148	**0.6051**	0.9586
Olefins	D1319	**0.1947**	0.2116	0.2980
Lubricity, Bocle	D5001	**0.0540**	0.0607	0.0618
Viscosity at 20 ºC	D445	**0.1364**	0.1424	0.1682
Viscosity at -20 ºC	D445	**0.0920**	0.1131	0.1114
Viscosity at -40 ºC	D445	**0.0996**	0.1349	0.1158
Acid number	D3242	0.6173	0.6135	**0.5459**
Thermal stability	D3241	0.1655	**0.1652**	0.2064
Mercaptan sulfur	D3227	0.9679	0.6527	**0.5378**
Sp. heat cap. at 0 ºC	E1269	**0.0597**	0.0734	0.0747
Conductivity	D2624	0.972	**0.8408**	1.0748
Acid number	D3242	0.6173	0.6135	**0.5459**
Distillation IBP	D86	**0.0303**	0.0345	0.0357
Distillation 10%	D86	**0.0164**	0.0265	0.0225
Distillation 50%	D86	0.0268	**0.0227**	0.0386
Distillation FBP	D86	0.0303	0.0349	**0.0292**

Table 10. Comparison of model performance according to analytical method used. Lowest RMSECV values for each property (normalized to mean property value) are listed in bold type.

It has also been shown that a key to successful chemometric analysis of complex chromatographic fuel data is the implementation of an ANOVA calculation performed at every time-resolved data point. This serves as a powerful feature selection utility to locate and extract chemically relevant data from much larger and complex GC-MS datasets. This extracted subset of relevant information was referred to in this paper as the feature selected data. PARAFAC analysis (a multi-way factor analysis algorithm) of the GC-MS data cube, after ANOVA feature selection, was shown, in principal, to be a successful route to elucidating chemical changes down to the individual compound level. This capability provides for a wide set of opportunities for significant improvements in fuel diagnostics and analysis. For example, by comparing GC-MS datasets from a fuel before and after thermal stress in this manner, it would be possible to obtain structural information on only those molecular species that changed in response to thermal stress. In principal, this will provide an excellent starting place to begin to characterize and/or validate likely mechanisms of fuel degradation. By coupling the chemometric algorithm's output to an electronic NIST mass spectrum database, it is possible to automatically generate a list of compounds that have either increased or decreased in concentration in response to a given

stimulus. The utility of this approach was demonstrated with two experiments, where compositional changes were detected in Naval distillate fuel during mild thermal stress, and how the evaporative losses were detected in vented bottle testing.

Chemometric analysis of a Naval distillate fuel subjected to thermal stress in the presence of catalytic copper, in a closed system, was shown to result in the same overall chemical composition as the same fuel stressed without copper. This indicated that in this instance, that while copper accelerated the autoxidation of the fuel, the reaction mechanisms to produce the final composition were similar as in the neat fuel.

Comparison of the GC-MS of an adulterated or blended fuel with that from the unadulterated fuel, can also provide an extremely sensitive identification of compounds in the adulterant or co-blended fuel. The feature selected chromatogram of the fuel adulterant can then be input to the appropriate PCA model to reveal the likely type of fuel that has been commingled with the original sample. This also can be used to selectively identify fuel adulterants that may have been added to the fuel either purposely or by accident, before acceptance for use. This was demonstrated in this study in the discrimination and quantification of trace levels of home heating oil, in a compositionally similar diesel fuel matrix.

5.2 Development of A Sensor-Based Fuel Quality Assessment Capability

A sensor-based fuel quality technology is based on relating a numerical representation of fuel composition, to the properties of interest. There are two major aspects to this approach; the type of sensor and its response to compositional features, and the chemometric models that predict the properties from the sensor data. In this study, we have demonstrated the feasibility of predicting of a number of critical fuel properties from compositional data. Reasonable property predictions were obtained from a small (46 sample) training set from capillary gas chromatography, NIR and Raman spectroscopy. The advantages of optical sensors over chromatographic devices for field use were discussed above, and thus the majority of this facet of the study was focused on spectroscopy.

In assessing the accuracy of the chemometric models to predict a particular fuel property, the most obvious way is to directly compare the predicted and measured values. However, the development of a global parametric measurement of error is complicated by the fact that the standard test methods to which the chemometric predictions are being compared to, also contain error. A common way to express the errors of prediction by a chemometric model is to compute the root mean square error of prediction (RMSEP) of a prediction subset of available data utilizing a model constructed from a separate "calibration" subset of data.[33] In this preliminary work, however, the training set consisted of only 46 jet fuel samples, necessitating model evaluation through "leave-one-out" cross validation, in which the prediction of a given sample is made utilizing a model generated from the remaining samples. Thus, when comparing predicted vs measured values for a property of interest, the root mean square error of cross-validation was used instead of the RMSEP. For the purpose of comparing the errors of prediction across the various fuel property models, the RMSECV values were normalized to the mean of the predicted values.

The results of this initial study were successful in producing models with RMSECV values for the critical fuel properties, i.e., flash point, density, freeze point, aromatics, and viscosity, that were less than 10% of observed mean property values within the training set used, and commensurate with uncertainties expected from the ASTM methods utilized to acquire reference

values for this study. This indicates that chemometric prediction of fuel properties from compositional data is feasible, although much more work must be done to validate the robustness of this approach as well as to develop rigorous implementation guidelines and requirements.

Comparison of GC, NIR and Raman spectroscopy indicates that a fuel quality sensor platform based on either NIR or Raman spectral data should perform acceptably, although GC could provide some improvement, particularly in the prediction of freeze point and viscosity. The prediction of fuel system icing inhibitor (FSII) remains to be predicted adequately by spectroscopy without any type of sample preparation. It appears that the structural features of the FSII additive (di-ethyleneglycol monomethyl ether) that are detectable by spectroscopy may not be sufficiently distinct from other fuel constituents to model chemometrically in fuel. Future studies will be directed towards the exploration of specialized mathematical treatments and potentially, alternate analytical methodologies to accomplish this. For example, a specialized chromatographic method, either alone or in combination with spectroscopy, may offer a pathway towards the successful direct measurement of FSII in jet fuel.

Taking this pathway a bit further, it is expected that data fusion techniques in which several types of analytical data can be combined in a single predictive model have the potential to offer distinct advantages over each measurement technique alone, in a manner analogous to the advantages offered by multivariate instrumentation (e.g. spectroscopy) over univarate instrumentation (e.g. single-point sensors). Thus, a model that combines both chromatography and spectroscopic data may be capable of accurately measuring FSII content, along with multiple other properties that are not currently amenable to chemometric modeling from spectroscopy alone. Taking this approach, the measurement of a broad range of fuel properties, including those that are not amenable to chemometric prediction from GC or NIR data, such as conductivity, total sulfur, and acid number, would in theory, be attainable with a NIR-based fuel quality assessment system that is augmented with a set of carefully chosen specialized sensors.

To achieve reliable, robust prediction of these properties in practice, a calibration set of fuels must be assembled that accurately reflects the span of levels at which each of these components is present in the range and type of fuels that are to be evaluated. Current work in this area is being undertaken to broaden the scope of the fuel training set. It is also a goal of this program to produce a stand-alone software implementation of these chemometric models, which would provide the means to export this to other fuel laboratories for use. The software would be constructed to so as to allow the user to update the models as new data are obtained.

A major caveat to these conclusions, however, lies in the limited nature of this feasibility study. Most of the fuel properties examined arise from complex interactions between many different fuel constituents. To achieve reliable, robust prediction of these properties in practice, a calibration set of fuels must be assembled that accurately reflects the span of levels at which each of these components is present in the range and type of fuels that are to be evaluated. Naturally, this leads to a requirement of hundreds, if not thousands of calibration samples to achieve predictions of high accuracy and precision, as well as to an implicit requirement that the instrumentation used to obtain the calibration data is of high reliability and precision. This phenomenon has been observed in work done by others in the prediction of octane number of gasoline via chemometric regression on NIR spectra. Thus, further work involving wider sample sets and increased replicates is required to fully ascertain the limitations of this method.

6.0 ACKNOWLEDGEMENTS

The authors wish to thank U.S. Naval Air Systems Command, Air 4.4.5, for supporting this work. They also wish to thank the following individuals for their assistance in acquiring fuel samples, specification data, spectra, and chromatographic data: Stan Seto (GE Aircraft Engines c/o Belcan Corporation), Jeffrey M. Johnson (Boeing Commercial Airplane Group), Wayne Smith (Real-Time Analyzers Inc.), Sherry Williams (Naval Air Systems Command), Richard Kamin, (Naval Air Systems Command), and Christina DiGiuilio (NOVA Research, Inc.)